Journal of Medicinal Chemistry Article

J. Med. Chem. **2009,** *52,* 4345–4357 **4345**
DOI: 10.1021/jm900225j

Synthesis, Binding, and Modeling Studies of New Cytisine Derivatives, as Ligands for Neuronal Nicotinic Acetylcholine Receptor Subtypes

Bruno Tasso,[†] Caterina Canu Boido,[†] Emanuela Terranova,[†] Cecilia Gotti,[‡] Loredana Riganti,[‡] Francesco Clementi,[‡] Roberto Artali,[§] Gabriella Bombieri,[§] Fiorella Meneghetti,[§] and Fabio Sparatore*[,†]

[†]*Dipartimento di Scienze Farmaceutiche, Università degli Studi di Genova, Viale Benedetto XV 3, 16139 Genova, Italy,* [‡]*Dipartimento di Farmacologia "E. Trabucchi", Università degli Studi di Milano, via Vanvitelli 32, 20129 Milano, Italy, Istituto di Neuroscienze del CNR, via Vanvitelli 32, 20129 Milano, Italy, and* [§]*Dipartimento di Scienze Farmaceutiche "P. Pratesi", Università degli Studi di Milano, Via Mangiagalli 25, 20133 Milano, Italy*

Received February 20, 2009

The availability of drug affecting neuronal nicotinic acetylcholine receptors (nAChRs) may have important therapeutic potential for the treatment of several CNS pathologies. Pursuing our efforts on the systematic structural modification of cytisine and *N*-arylalkyl and *N*-aroylalkyl cytisines were synthesized and tested for the displacement of [^{3}H]-epibatidine and [^{125}I]-α-bungarotoxin from the most widespread brain nAChRs subtypes $\alpha_4\beta_2$ and α_7, respectively. While the affinity for α_7 subtype was rather poor (K_i from 0.4 to $> 50\,\mu$M), the affinity for $\alpha_4\beta_2$ subtype was very interesting, with nanomolar K_i values for the best compounds. The N-substituted cytisines were docked into the rat and human $\alpha_4\beta_2$ nAChR models based on the extracellular domain of a molluscan acetylcholine binding protein. The docking results agreed with the binding data, allowing the detection of discrete aminoacid residues of the α and β subunits essential for the ligand binding on rat and human nAChRs, providing a novel structural framework for the development of new $\alpha_4\beta_2$ selective ligands.

Introduction

Neuronal nicotinic acetylcholine receptors (nAChRs[a]) form a family of pentameric ACh-gated cation channel, made up of different subtypes, each of which has a specific pharmacology, physiology, and anatomical distribution in brain and ganglia.[1,2] They are widely distributed in peripheral and central nervous systems, where they act as postsynaptic receptors exciting neurons, or as presynaptic receptors modulating the release of many neurotransmitters. Neuronal nAChRs are involved in complex cerebral processes as learning, memory consolidation, nociception, locomotor activity, as well as in a growing number of degenerative diseases (Alzheimer's and Parkinson's diseases) and nervous pathologies such as autism, ADHD, anxiety, and schizophrenia. Thus they are interesting targets for the treatment of a variety of CNS disorders, particularly Alzheimer's and Parkinson's diseases, opiate resistant chronic pain, and tobacco smoking addiction, which may involve specific nicotinic receptor subtypes, among which $\alpha_4\beta_2$ is the most abundant in the brain.[3−5] Each of the nAChR subunits displays a characteristic phenotype of structural features extending from the N-terminus to the C-terminus: (1) a large (∼200 amino acids) N-terminal hydrophilic domain containing the multiple loops of the neurotransmitter binding site, (2) the highly variable C-terminal hydrophilic domain that is extracellular, and (3) a set of four closely spaced transmembrane domains (termed M1−M4) immediately following the large extracellular domain. The M2 domain is believed to form the wall of the ion channel. The loops that comprise the agonist binding site contain conserved residues, many of which possess aromatic side chains (Trp and Tyr), which are proposed to make cationic−π interactions with agonists.[1]

The achievement of subtype selective agents that can bind and modify the function of nAChRs has been attempted mainly by structural modification and synthesis of analogues of nicotine and epibatidine, two very potent natural agonists (Chart 1). A large number of compounds have been prepared and tested,[6−8] but only a few of them exhibited promising characteristics, particularly tebanicline (5-[(2*R*)-2-azetidinylmethoxy]-2-chloropyridine; ABT-594) as an analgesic[9] and ABT-418 ((*S*)-3-methyl-5-(1-methyl-2-pyrrolidinyl)isoxazole) as a cognition enhancing agent.[10] However, for both compounds, the clinical trials have been discontinued due to adverse effects. Another important nicotinic agonist, which could disclose new perspective and opportunities for developing new agonists and/or antagonists, is represented by cytisine (**1**), an alkaloid mainly obtained from seeds of *Laburnum anagyroides* but present also in several other plants of the Leguminosae family, to which it confers intoxicant properties. Until recently, Texas Mountain Laurel, also known as mescal beans (*Sophora secundiflora*), was believed to have been used as a divinatory medium even prior to the discovery of peyote by many American Indian tribes of the South West.[11] Despite the name, mescal beans do not contain mescaline but cytisine

*To whom correspondence should be addressed. Phone: +39-010-3538359. Fax: +39-010-3538358. E-mail: sparator@unige.it.

[a]Abbreviations: AA, amino acid; ACh, acetylcholine; AChBP, acetylcholine binding protein; ADHD, attention deficit hyperactivity disorder; AMBER, assisted model building with energy refinement; CC, column chromatography; CNS, central nervous system; CPK, Corey−Pauling−Koltun; CV, coefficient of variation; MM, molecular mechanical; nAChRs, nicotinic acetylcholine receptors; NPT, normal pressure and temperature; PDB, protein data bank; QM, quantum mechanical; rmsd, root-mean-square deviation; SMP CPU, symmetric multiprocessing central processing unit; TRIS·HCl, tris(hydroxymethyl)aminomethane hydrochloride.

Published on Web 06/23/2009

Chart 1

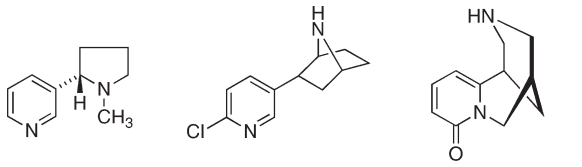

(-)-(*S*)-Nicotine (±)-Epibatidine (-)-(7*R*,9*S*)-Cytisine (**1**)

and other related lupine alkaloids. Cytisine showed very high affinity for nAChRs[12] and is able to discriminate among some subtypes, with a higher affinity for $\alpha_4\beta_2$ than $\alpha_3\beta_4$ *s*ubtype.[13] Preference for $\alpha_4\beta_2$ versus $\alpha_3\beta_4$ subtype has been observed also for N-substituted cytisine derivatives.[14]

Alhough the pharmacological profile of cytisine has been thoroughly studied,[15] this alkaloid has not found any therapeutic application in western countries, while in the former Soviet Union it was preferred to lobeline as a respiratory analeptic[16] and was used to treat tobacco dependence for the last 40 years in several East European Countries.[17] Only recently cytisine has received some attention as a lead for structural analogues or derivatives able to interact, directly or allosterically, with one or more nAChR subtypes. Four patents[18−20] suggested hypoglycemic, anti-inflammatory, antiaddiction, and neuroprotective activities for cytisine, its *N*-methyl (cauliphylline), and pyridone-substituted derivatives. Recently Canu Boido and Sparatore[14,21−24] prepared and assayed in a number of tests a variety of cytisine derivatives with substitution in the pyridone ring or N-substituted. Afterward, several authors addressed their interest to the study of different cytisine derivatives with substitution in the pyridone ring or with N- or C-substitutions on the bispidine moiety.[25−30] Finally, Coe et al.,[31] through a progressive modification of the molecular frame of cytisine obtained varenicline (6,7,8,9-tetrahydro-6,10-methano-6*H*-pyrazino-[2,3-*h*][3]benzazepine), which displayed high binding affinity and selectivity for rat $\alpha_4\beta_2$ subtype and an interesting therapeutic potential for smoking cessation and treatment of alcohol dependence.

In line with these studies, we continue the investigation on additional N-substituted derivatives of cytisine mainly because the introduction of substituents on cytisine amino group still represent the simplest way to enhance the molecular lipophilicity and improve passage through cell membranes and the blood−brain barrier. Although the N-substitution is commonly considered detrimental for affinity to nAChRs, the increased lipophilicity could balance this negative effect.

To contribute to the understanding of the structural requirements for targeting the nAChRs we have: (A) synthesized several *N*-[(ω-aryl/heteroaryl)alkyl]cytisines and *N*-(ω-aroylalkyl)cytisines (**2**−**23**) and, for comparison, a few cytisine derivatives bearing aliphatic substituents (**24**−**29**) (Chart 2) that were assayed for the displacement of [^{3}H]-epibatidine and [^{125}I]-bungarotoxin from $\alpha_4\beta_2$ and α_7 receptor subtypes of rat cortex,[1b] respectively. Both these subtypes have been proposed as therapeutic targets for neurological pathologies and degenerative diseases. (B) In view of the observed higher affinity for $\alpha_4\beta_2$ versus α_7 subtypes, we docked the N-substituted cytisines in the structural model of the nAChRs extracellular ligand binding domain of the rat $(\alpha_4)_2(\beta_2)_3$ type (PDB code: 1OLE), as well as in our human $(\alpha_4)_2(\beta_2)_3$ type (PDB code: 2GVT), developed through homology modeling techniques based on the X-ray structure of the *Aplysia californica* AChBP (PDP code: 2BYQ).[32,33]

Results and Discussion

Chemistry. The cytisine derivatives **2**, **3**, **6**, **9**, **12**, **19**, **23**, **27**, and **29** were already described by Canu Boido and Sparatore.[21] The novel *N*-arylalkyl and aroylalkyl derivatives **7**, **8**, **13**, **14**, **16**−**18**, **20**−**22**, and the *N*-(4-oxopentyl)cytisine **28** were obtained by reacting cytisine with the suitable haloderivatives in a ratio 2:1. For preparation of *N*-[(pyridin-3/4-yl)-methyl]− and *N*-[3-(pyridin-3-yl)propyl]cytisines (**4**, **5**, **15**), an excess of cytisine was reacted with the relevant bromoalkylpyridine hydrobromide. It is worth noting that it was impossibile to obtain the *N*-[(pyridin-2-yl)methyl]cytisine because the 2-bromomethylpyridine reacted with itself as soon it was liberated from the hydrobromide.

To obtain compound **24**, cytisine was reacted with iodoacetamide in the presence of anhydrous K_2CO_3. The preparation of 2- and 4-pyridylethyl (**10**, **11**), carbamoylethyl (**25**), and methylsulfonylethyl-derivative (**26**) was effected through a Michael addition of cytisine on the corresponding unsaturated compounds (2- and 4-vinylpyridine, acrylamide, and methyl-vinylsulfone) (Scheme 1). The structures of the prepared compounds were supported by elemental analyses and spectral data.

In Vitro Receptor Binding. The results of the binding assay of cytisine (**1**) and its N-substituted derivatives **2**−**29** on $\alpha_4\beta_2$ and α_7 rat receptor subtypes are collected in Table 1. Most compounds exhibited very poor affinity to α_7 subtype, often more than 100-fold lower than cytisine, with K_i > 50000 nM. Only two compounds (**20**, **21**) showed a K_i value rather close to that of cytisine (K_i = 331 nM). On the other hand, according to their affinity toward $\alpha_4\beta_2$ subtype, the tested compounds can be grouped in three clusters: (a) eight compounds with high affinity (K_i = 2.6−63 nM), (b) 13 with moderate affinity (K_i = 330−965 nM), and (c) seven with poor affinity (K_i = 1300−13000 nM).

Binding studies for cytisine and 12 of its derivatives were also performed in rat cortex $\alpha_4\beta_2$ receptor subtype labeled with [^{3}H]-cytisine. The observed K_i values (see Supporting Information) are well concordant with those of Table 1 ([^{3}H]-epibatidine displacement).

The reasons for the differences in the observed binding affinity can depend from the interplay of the following structural features:

(i) the length of the aliphatic chain that is interposed between the basic nitrogen and the aromatic ring: one C (**2**−**5**), two C (**6**−**11**, **18**, **19**), three C (**12**−**15**, **20**, **21**), four C (**16**, **17**, **22**, **23**);

(ii) the presence of an electron withdrawing group (carbonyl, sulphonyl) in the chain and its distance from the basic nitrogen (**18**−**28**);

(iii) the presence and the nature of substituents on the aromatic moiety.

With an unsubstituted benzene nucleus, the elongation of the aliphatic chain has a fluctuating effect, improving and then decreasing the affinity: *N*-phenylethyl− and *N*-phenylpropylcytisine have an affinity more than 1 order of magnitude higher than *N*-benzyl− and *N*-phenylbutylcytisine. On the contrary, in *N*-(4-fluorophenyl)alkylcytisines, the affinity decreases steadily with the increasing number of methylene groups. Evidently, the *para*-fluoro

Chart 2

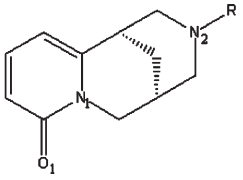

	R		R
1	H (Cytisine)	**16**	$(CH_2)_4$-C_6H_5
2	CH_2-C_6H_5	**17**	$(CH_2)_4$-C_6H_4-F(4)
3	CH_2-C_6H_4-F(4)	**18**	CH_2-CO-C_6H_5
4	CH_2-3-pyr	**19**	CH_2-CO-C_6H_4-F(4)
5	CH_2-4-pyr	**20**	$(CH_2)_2$-CO-C_6H_5
6	$(CH_2)_2$-C_6H_5	**21**	$(CH_2)_2$-CO-C_6H_4-F(4)
7	$(CH_2)_2$-C_6H_4-F(4)	**22**	$(CH_2)_3$-CO-C_6H_5
8	$(CH_2)_2$-C_6H_4-CH_3(4)	**23**	$(CH_2)_3$-CO-C_6H_4-F(4)
9	$(CH_2)_2$-C_6H_4-OCH_3	**24**	CH_2-CO-NH_2
10	$(CH_2)_2$-2-pyr	**25**	$(CH_2)_2$-CO-NH_2
11	$(CH_2)_2$-4-pyr	**26**	$(CH_2)_2$-SO_2-CH_3
12	$(CH_2)_3$-C_6H_5	**27**	$(CH_2)_2$-CO-CH_3
13	$(CH_2)_3$-C_6H_4-F(4)	**28**	$(CH_2)_3$-CO-CH_3
14	$(CH_2)_3$-C_6H_4-CH_3(4)	**29**	$(CH_2)_4$-CH_3
15	$(CH_2)_3$-3-pyr		

Scheme 1[a]

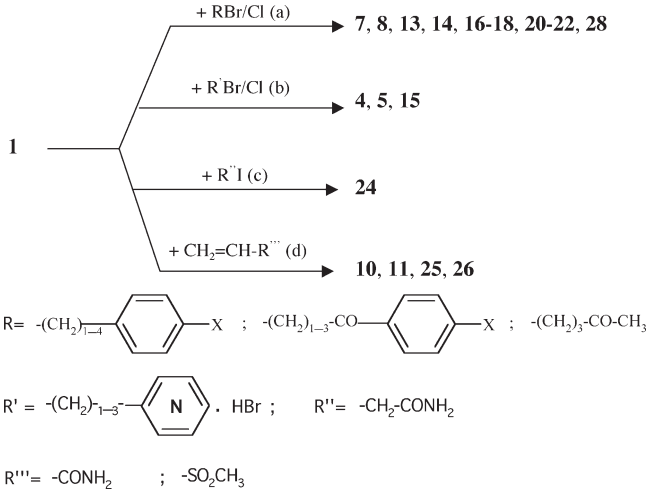

[a]Reagents and conditions: (a) ratio **1**: RBr/Cl = 2:1; MeCN; 90−100 °C; 20−24 h; (b) ratio **1**: R′Br = 3:1; MeCN; 100 °C; 36 h; (c) ratio **1**: R″I = 1:1; K_2CO_3; 100 °C, 7 h; (d) ratio reactants = 1:1; EtOH; AcOH; reflux, 24 h.

substitution improved a little the affinity of the benzyl derivative but strongly lowered that of phenylethyl− and phenylpropyl− derivatives. A similar deleterious effect was observed also for the 4-methyl and 4-methoxy substitution. The replacement of the benzene ring with the pyridine affected the affinity depending on the joining position: the 4-pyridylmethyl− and the 4-pyridylethylcytisines (**5** and **11**) behaved similarly to the corresponding phenyl derivatives (**2** and **6**), while the 2- and 3-pyridylalkyl derivatives (**4**, **10**, and **15**) exhibited a reduced affinity with respect to **2**, **6**, and **12**.

Table 1. Binding Affinity (K_i, nM) of Compounds **1**−**29** to $\alpha_4\beta_2$ and α7 Rat Nicotinic Receptor Subtypes, Labeled with [^{3}H]-Epibatidine and [^{125}I]-Bungarotoxin, Respectively[a]

	K_i, nM (%CV)			K_i, nM (%CV)	
	$\alpha_4\beta_2$	α_7		$\alpha_4\beta_2$	α_7
1	0.48(20)	331(28)	**16**	3900(29)	nd
2	850(20)	> 50000	**17**	13000(26)	> 50000
3	330(21)	78700(50)	**18**	17(32)	2250(26)
4	6600(30)	> 100000	**19**	409(30)	nd
5	675(27)	> 100000	**20**	2.6(23)	550(22)
6	28(28)	25000	**21**	5.3(18)	433(22)
7	1300(25)	> 50000	**22**	816(30)	> 50000
8	727(29)	> 50000	**23**	965(27)	> 50000
9	495(24)	> 50000	**24**	7300(30)	> 50000
10	941(32)	> 100000	**25**	35(31)	3600(38)
11	7.2(26)	4200(29)	**26**	564(24)	> 50000
12	63(17)	13000(17)	**27**	8.7(24)	1240(22)
13	5000(35)	> 50000	**28**	757(29)	> 50000
14	7200(26)	> 50000	**29**	332(22)	39700(20)
15	744(37)	> 100000			

[a]The K_i values shown were the mean (% coefficient of variation) of three-six independent measurements.

The introduction of a carbonyl group on the connecting aliphatic chain (**18**−**23**) had always a positive influence on affinity, but this effect became outstanding when the carbonyl was in the β-position with respect to the basic nitrogen (**20**, **21**), also overcoming the negative influence of the *para*-fluoro substitution. This observation still holds in the case of compounds devoid of an aromatic ring, such as **25** and **27**, and suggests the possibility that all these compounds could undergo to β-elimination reaction during the overnight incubation, with release of cytisine, to which should be due the displacement of the labeled ligand. However the release of cytisine in the binding experimental conditions must be

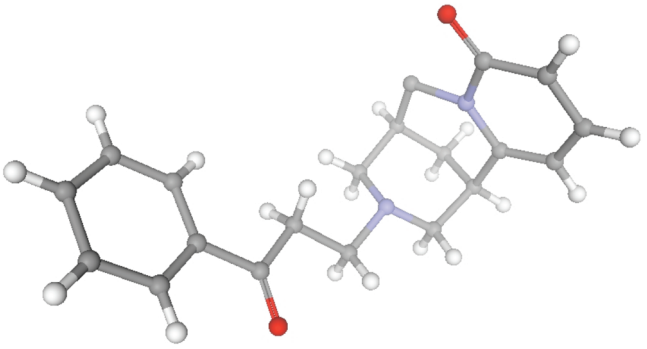

Figure 1. Crystal structure of one of the two independent molecules of **20** (color by atom type: gray, carbon; blue, nitrogen; red, oxygen; white, hydrogen).[34].

ruled out because the *N*-(benzoylethyl)cytisine, one of the best ligands versus both $\alpha_4\beta_2$ and α_7 subtypes, was recovered unchanged even after prolonged incubation in the usual buffer solution. Thus the observed high affinity is peculiar to compounds **20**, **21**, **25**, and **27**, which together with compounds **6**, **11**, and **18** are the most interesting of the whole set. The ratio between the affinity constants of compounds **25** and **20** was 13.46, while that between the corresponding lower homologues **24** and **18** was 429.4; therefore, when the carbonyl group is placed in β position to the basic nitrogen, the NH_2 group exerts only a minor negative influence, while in the shorter chain, it probably prevents the correct positioning of the ligand on the receptor.

Molecular Docking. With the aim to a better understanding of the influence of the N-substitution at the cytisine system in the new synthesized compounds, we have examined the lower energy docking pose of cytisine (the reference compound) in the binding pockets of rat and human nAChRs. In both models, we have found the protonated nitrogen lying in the center of the "aromatic cluster" formed by the aromatic residues present at the ligand binding pocket.[32] In the rat receptor model, the pyridone stacks onto Phe117 and the pose is stabilized by a H-bond with OTrp147, while in the human model the charged nitrogen is sandwiched between Trp55 and Tyr195 and a hydrogen bond involving the pyridone oxygen and NHETrp147 is present.

A detailed presentation of AA forming the rat and human binding sites of the receptor is given as Supporting Information, Table S2.

Before discussing separately the docking of the 28 cytisine derivatives on the rat and human receptor models, it is important to observe that in both models the charged nitrogen of the N-substituted derivatives is inside the aromatic cage, but the cytisine pyridone ring points toward the α subunit, in opposite direction with respect to the other compounds, in which the pyridone ring is directed toward the β subunit. The constantly higher affinity of the unsubstituted alkaloid might be related to this different orientation inside the binding pocket.

Rat $(\alpha_4)_2(\beta_2)_3$ nAChRs. The X-ray structure of **20**[34] that exhibits the highest affinity has been used for molecular docking analysis.

In its neutral form, **20** is represented by two independent molecules with the same conformation of the cytisine moiety with the pyridone ring almost planar, the adjacent ring in envelope conformation, and the "bispidine" scaffold in chair conformation (Figure 1).

The minimum energy conformation of the examined compound based on this model give rise to several docking conformations, which after a visual inspection were clustered and further analyzed through hybrid QM/MM geometry optimization. Hybrid QM/MM methods have become a standard tool for the characterization of complex molecular systems, as permitted to analyze quantum mechanically the fraction of the system that undergoes to the most significant changes during the substrate binding, while the rest of the system has been simulated with the traditional molecular mechanic methods. This process was used to rerank the structures generated by docking and to simulate the structural adaptations occurring in the ligand−receptor binding. First, the more relevant docked conformations of the complex ligand−rat $(\alpha_4)_2(\beta_2)_3$ were equilibrated for 1.5 ns by molecular dynamics, at constant temperature and pressure in a periodic cubic box, using the TIP3P model for water molecules (results not shown). The systems were subsequently optimized using the combined QM/MM approach, with a flexible receptor environment allowing simulation of the modification of the receptor upon ligand binding. This procedure gives rise to a rearrangement of the residues forming the binding site around the ligand ("induced fit"), leading to the situation showed in Figure 2 for **20**.

This binding site optimization leads to a small difference in the residue geometry with respect to the starting conditions (rmsd all atoms of 1.08 Å), while the number of hydrogen bonds and ligand−residue contacts are almost unaffected.

The binding of **2**−**29** is characterized by hydrogen bonds and/or cation−π interactions, with the protonated cytisine nitrogen oriented toward the aromatic cage of the binding pocket. The presence of a hydrogen bond between the hydrogen of the protonated piperidine nitrogen N_2 (arbitrary numbering, see Chart 2) and the macromolecule is a stabilizing factor for the orientation of the ligands. Although the majority share the same cation−π interaction with the receptor, others adopt a somewhat diverse orientation within the binding pocket with different interaction patterns. The best score binding pose of the most potent compound **20** presents two hydrogen bonds: the protonated amine moiety (N_2H) interacts with the Trp147 backbone oxygen at the distance of 2.69 Å, while the ketonic oxygen is 2.40 Å apart from OHTyr195. The cytisine pyridone is sandwiched in the aromatic cage, with the side chain pointing toward the α4 subunit. The binding mode of **20** to rat $(\alpha_4)_2(\beta_2)_3$ nAChR model is shown in Figure 3 (left). The derivative **21** follows the same behavior of compound **20**. The introduction of a fluorine atom gives rise to a comparable conformation of the side chain and of the cytisine moiety, determining however two hydrogen bonds between the protonated amine moiety (N_2H) and the Trp 147 backbone oxygen at the distance of 3.00 Å and between the pyridone oxygen O_1 with NHTyr195 at 2.08 Å, without any interaction between O_2 and HOTyr195. Compounds **18**, **25**, and **27**, all bearing a carbonyl group in the side chain but largely differing for the terminal moiety, share the interaction pattern of **21**. It is worth noting that the docking free energy value of compound **25** ranks higher than expected on the base of the experimental data.

The influence of the pyridine nitrogen in compounds **10** and **11** shows that the shifting from the 4-position to the 2-position in **10** leads to a significant decreasing in affinity. These two compounds dock in a quite similar orientation as shown for **10** in Figure 3 (right), but compound

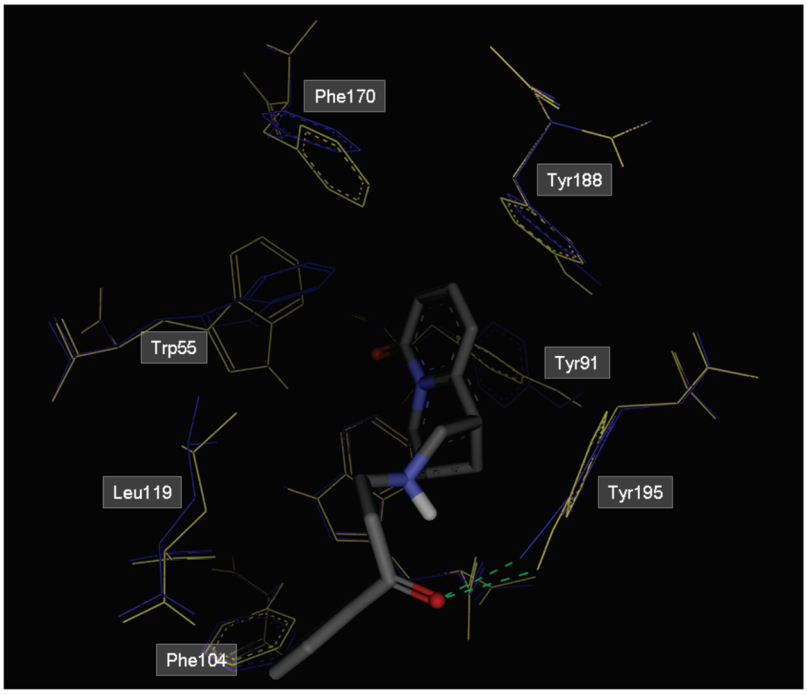

Figure 2. Particular of the QM region used in the QM/MM optimization of the rat receptor model and the **20** bioactive conformation in stick (CPK). Residues in the starting conformation in blue sticks and after the QM/MM optimization in yellow sticks.

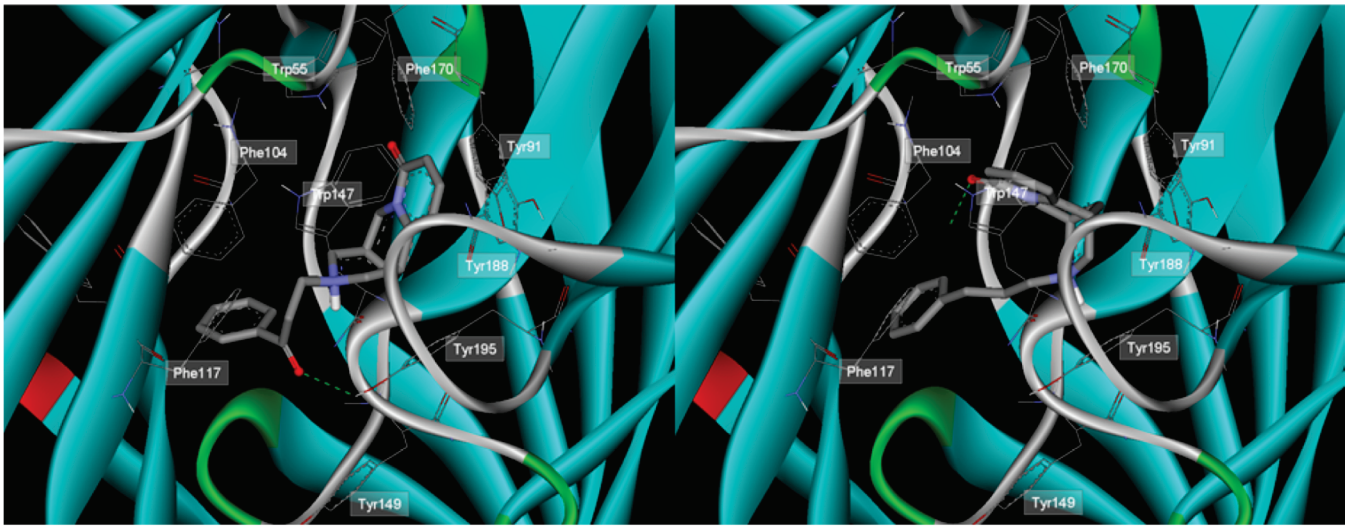

Figure 3. Representation of the best docked conformations rendered in capped sticks of **20** (left) and **10** (right) into the ligand-binding domain (lines). Putative intermolecular hydrogen bonds are highlighted by green dashed lines.

11 has a higher consensus score in agreement with its better affinity (Table 1).

Independently from the length and the nature of the side chain, compound **12**, as well **2**−**5**, **7**−**10**, **14**−**17**, **19**, **22**−**24**, **26**, **28**, and **29**, present a productive cation−π interaction between the protonated amine moiety (N_2H) and Trp147 (average distance 3.9 Å). For these compounds, with the exception of the most extended molecules, the different orientations of the cytisine moiety still allow the formation of one H-bond between the protonated amine moiety (N_2H) and the Trp147 backbone oxygen.

The introduction of the fluorine atom in 4-position in compound **13** produces a 2 orders of magnitude decrease in affinity with respect to **12**, and this fact could be justified by the fluorine atom repulsion with the backbone nitrogen of Leu119, giving rise to a different orientation of the side chains (Figure 4). Similarly, all the most extended molecules hardly fit in the binding pocket and those devoid of a carbonyl group in the chain (**14**, **16**, and **17**) can have only very poor interactions with the receptor.

In general, with the exception of compound **3**, the docking calculations evidence that the 4-substitution in the aromatic moiety accounts for a worse interactions between the aromatic macromolecular moieties and the ligand, lowering the consensus score. This effect is, however, overwhelmed by the insertion of a carbonyl group which hydrogen bonds residues in the binding pocket, as observed, for example, in the case of the most extended and least potent compound **17** (ΔG = 7.02 kcal/mol) and the corresponding ketone **23** (ΔG = 9.55 kcal/mol, see Table 2).

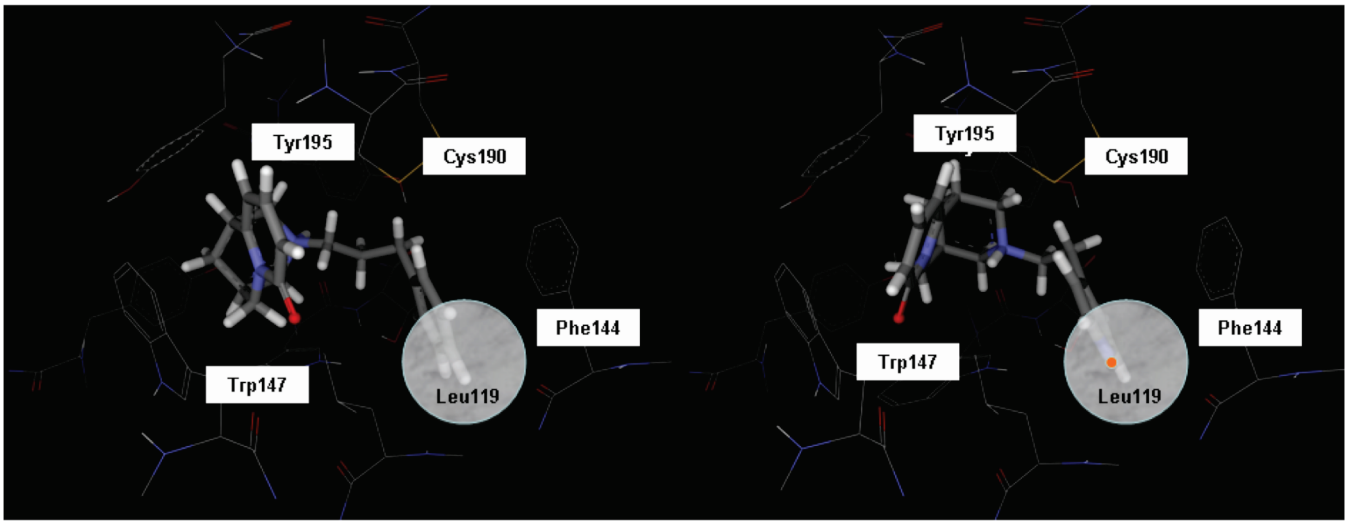

Figure 4. Representation of the best docked conformations rendered in capped sticks of **12** (left) and **13** (right) into the ligand-binding domain of rat model (lines). The highlighted region evidence the Leu119 position with the **13** fluorine atom as orange spot. Putative intermolecular hydrogen bonds are represented by green dashed lines. No C−F···HN bond is present.

Table 2. Best Docking Scores of Cytisine and Derivatives **2**−**29** for Rat and Human $(\alpha_4)_2(\beta_2)_3$ nAChRs Models Compared with Experimental Data[a]

	ΔG_{exp}	ΔG_{dock} rat	ΔG_{dock} human		ΔG_{exp}	ΔG_{dock} rat	ΔG_{dock} human
1	−12.71	−12.66	−12.82	**16**	−7.38	−7.13	−7.02
2	−8.28	−9.12	−10.62	**17**	−6.67	−7.02	−8.62
3	−8.84	−9.99	−10.94	**18**	−10.60	−10.33	−12.16
4	−7.07	−8.12	−9.63	**19**	−8.72	−9.21	−9.29
5	−8.42	−8.02	−11.02	**20**	−11.71	−11.81	−12.48
6	−10.30	−10.10	−12.10	**21**	−11.29	−11.78	−12.41
7	−8.03	−9.11	−10.21	**22**	−8.31	−9.14	−10.62
8	−8.37	−7.91	−10.94	**23**	−8.21	−9.55	−10.24
9	−8.60	−9.31	−8.17	**24**	−7.01	−7.98	−9.14
10	−8.22	−9.11	−9.45	**25**	−10.17	−10.99	−12.08
11	−11.11	−11.46	−12.31	**26**	−8.53	−9.45	−11.19
12	−9.82	−10.13	−11.98	**27**	−11.00	−10.49	−12.28
13	−7.23	−6.87	−8.96	**28**	−8.35	−8.87	−8.73
14	−7.02	−8.45	−8.78	**29**	−8.84	−8.45	−8.83
15	−8.36	−8.17	−10.87				

[a] ΔG values are in kcal/mol.

The destabilizing influence of the halogen substitution and the possible repulsive interactions lead to a detrimental binding, as previously reported in our docking study on the AChBP with 6-chloropyridazin-3-yl derivatives.[35]

Human $(\alpha_4)_2(\beta_2)_3$ nAChRs. With the aim to have new tools for predicting the binding affinities of the studied compounds for the human receptor type, compounds **2**−**29** were docked in our human $(\alpha_4)_2(\beta_2)_3$ nAChR model. Its amino acid sequence is highly conserved (overall rmsd 0.9 Å). Main differences are in the β subunit, in particular in the range 99−104 (Figure 5).

In the compounds **2**, **4**, **8**−**13**, **15**, **16**, **18**−**21**, **26**, and **29**, the piperidine NH makes an hydrogen bond with the macromolecule. Although most of them share the same cation−π interaction with the receptor, others adopt a distinct orientation within the binding pocket with different interactions. The best binding pose of **20**, shown in Figure 6 (left), is again characterized by two hydrogen bonds between the protonated amine moiety (N_2H) with Trp147 backbone oxygen at the distance of 2.10 Å and between the ketonic oxygen with

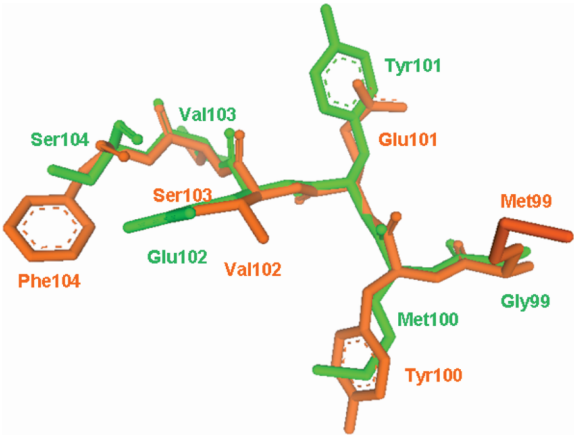

Figure 5. Superimposition of the nonconserved residues of the human (green) and rat (red) $(\alpha_4)_2(\beta_2)_3$ nAChR models in the range 99−104.

OHTyr195 at 2.35 Å. The cytisine pyridone ring is sandwiched in the aromatic cage between Tyr195 (centroid distance 4.2 Å) and Tyr188 (centroid distance 3.9 Å). The side chain points toward the α4 subunit and the benzene moiety stacks nearly parallel to the Phe117 aromatic ring at about 4 Å (centroid distance). For compound **21**, the introduction of a fluorine atom generates a different conformation of the side chain modifying the π interaction of the cytisine moiety, which results less deeply positioned within the aromatic cage. The decreasing of these π interactions lowers the consensus score, nevertheless **21** forms one hydrogen bond between O_1···NHETrp147 at 2.26 Å (Figure 6 right).

The shortening of the side chain of **20**, to give compound **18**, produces several changes in the docking. The cytisine system is linked by the charged nitrogen to NHCys190 at 2.34 Å and its aromatic heterocycle lies parallel to Trp147 and to Tyr188 (centroid distances 4.1 and 4.6 Å, respectively). These contacts do not influence the stacking of the aromatic moiety of the chain, which is 4.2 Å apart from the Phe117 aromatic ring. However, the ketone carbonyl strongly hydrogen bonds to NHETrp147 (1.99 Å) and to HOThr148 (2.8 Å) instead of OHTyr195 as observed for **20**.

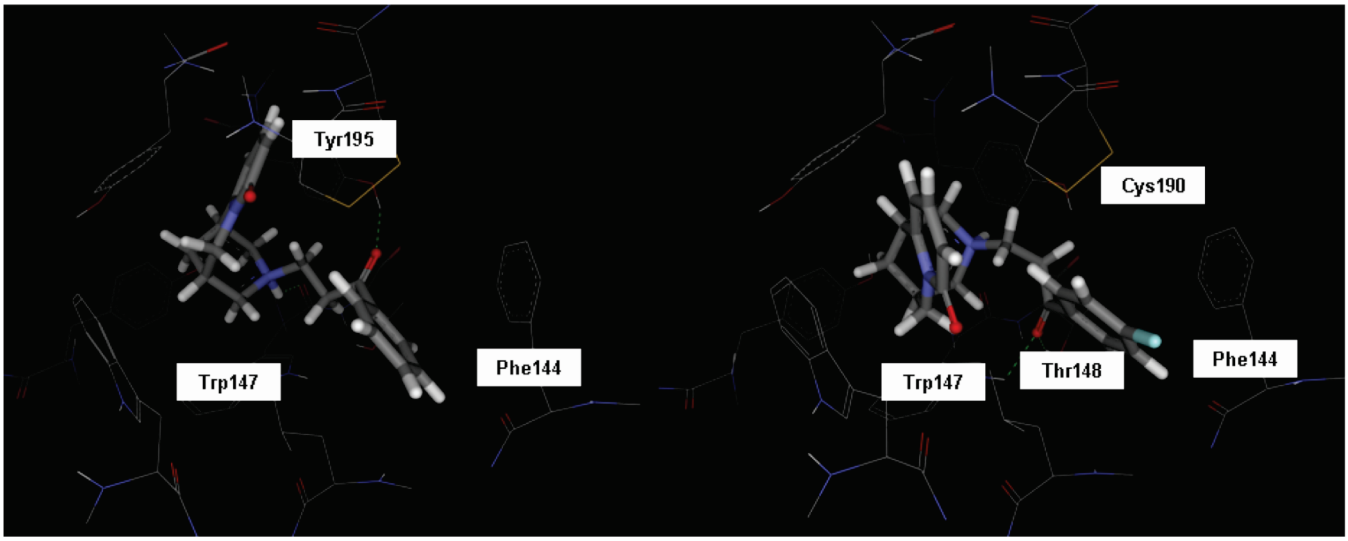

Figure 6. Representation of the best docked conformations rendered in capped sticks of **20** (left) and **10** (right) into the human ligand-binding domain (lines). Putative intermolecular hydrogen bonds are highlighted by green dashed lines.

The exchange of the ketone group for a methylene in **20** and **18** gives rise to the phenylpropyl− (**12**) and the phenylethyl− (**6**) derivative respectively, with a decrease of affinity that is stronger in the first case (K_i from 2.6 to 63 nM) than in the second one (K_i from 17 to 28 nM).

The phenylpropyl derivative **12** presents a tight interaction of the cytisine ring system with the receptor, characterized by the strong hydrogen bond of piperidine N_2H with NHETrp147 at 2.08 Å and of O_1 with NHCys190 at 2.35 Å. This system is further stabilized by a stacking interaction of pyridone ring with Tyr188 at 3.9 Å and of the terminal phenyl ring over Phe117.

For compound **13**, the repulsion between the para fluorine atom and the Gln58 carbonyl oxygen could influence the receptor affinity, as it was in rat model, with respect to **12**. The orientation of **12** is retained in the lower homologue **6**, which despite the shorter side chain maintains the productive π interactions with Trp147 and Phe117. The phenylethyl derivative **6** is the only one which presents, as best score pose, the cytisine oxygen engaged in a hydrogen bond with NHCys191 at 2.35 Å, while the pyridone ring is yet closely packed to Tyr195 and Tyr188 at about 4.01 Å distance, as seen for compound **20**.

The passage from **20** and **21** to compound **11**, despite the major structural changes (absence of ketone group, shorter linker, and pyridine in place of the benzene ring) leads to a quite equipotent derivative, but the interactions at the binding site are rather different. The piperidine NH of this compound hydrogen bonds with OTrp147 at 3.05 Å, and this interaction is reinforced by the good fit of the cationic head into the aromatic-rich binding pocket and by two favorable π interactions of the pyridone ring with the aromatic side chain of Tyr188 (centroid distance 4.1 Å) and of the pyridine with Phe117 at 4.8 Å distance.

The isomeric compound **10** has a similar orientation as **11** in the human model docking, but despite the presence of the stabilizing hydrogen bonds between the pyridine nitrogen and NHETrp147 and HOThr148, presents a lower consensus score than **11**. Thus, the 2 orders of magnitude decrease of affinity, due to the shift from 4- (**11**, K_i = 7.2 nM) to 2-pyridine substitution (**10**, K_i = 941 nM), remains hard to explain.

The substitution of the aromatic ring of the side chain with smaller groups as for **25** and **27** do not change the position of the cationic cytisine inside the human aromatic binding pocket and allows the formation of additional hydrogen bonds. In particular, in **25**, the amide is strongly linked to HNCys191 and to OGlu189 with the nitrogen and to HNCys191 with the oxygen, while in **27**, the carbonyl group hydrogen bonds HOTyr195, increasing its consensus score. The comparison of the molecular docking results of compounds **24** and **25** evidence novel discriminating receptor interactions, unexpected considering their small chemical diversity. The addition of a methylene group in **25** side chain allows the formation of two hydrogen bonds involving the cytisine protonated nitrogen, which can be considered, also in the light of this finding, important to elicit the nicotinic activity. The **25** amidic moiety leads to unfavorable electronic interactions with respect to the phenyl group of **20**, which shows about 15-fold higher affinity in rat receptor.

Concluding, the eight compounds with the highest affinity (**20**, **21**, **11**, **27**, **18**, **6**, **25**, and **12**, in order of decreasing affinity: K_i from 2.6 to 63 nM) behave similarly in both rat and human receptor models and exhibit docking free energy values that parallel the experimental ones, with the only exception of compound **25**, which ranks higher than expected in rat model.

The parallelism between the experimental affinity data and the docking free energy values is partially upset for compounds of the groups with moderate (K_i = 330−965 nM) and poor (K_i = 1300−13000 nM) affinity, in particular for that concerning the human model. The most striking deviation is observed for compound **9**, which ranks as the last but one in the human model, while it displays a moderate affinity (K_i = 495 nM) in the binding experiments.

The statistical analysis of the docking scoring functions point out the higher quality for the rat model with respect to human $(\alpha_4)_2(\beta_2)_3$ (Table 2 and Figure 7): an expected result, taking into account that the pharmacological data are for rat receptor. In particular, the correlation coefficient calculated between ΔG_{exp} and ΔG_{dock} is the most relevant element for the model quality assessment, which is 0.85 for the rat model and 0.67 for the human model, as shown by the obtained

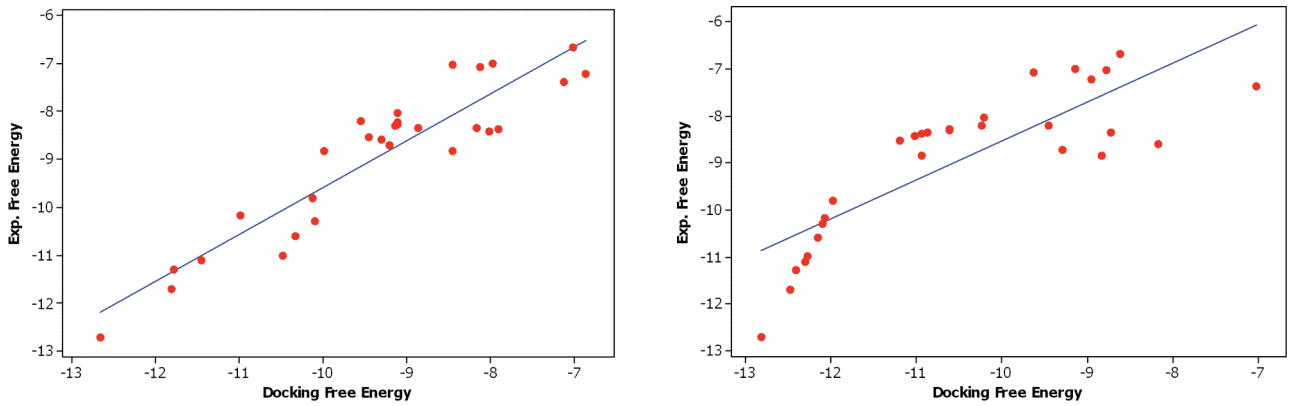

Figure 7. Correlation between the experimental (ΔG_{exp}) and docking (ΔG_{dock}) free energies calculated in ligand-binding [GB1]domain of rat (left) and human (right) $(\alpha_4)_2(\beta_2)_3$ nAChR model.

linear regression equations:

$$\Delta G_{exp} = 0.220 + 0.981 \Delta G_{model}$$

$$n = 29 \quad r^2 = 0.85 \quad q^2 = 0.85 \quad s = 0.61 \quad F = 156.03$$

$$\Delta G_{exp} = -0.25 + 0.829 \Delta G_{model}$$

$$n = 29 \quad r^2 = 0.68 \quad q^2 = 0.67 \quad s = 0.91 \quad F = 57.33$$

In the light of these findings, the close analogy between the same receptor subtype $\alpha_4\beta_2$ of the two species and the rather similar docking interactions permit consideration of our human receptor model useful to predict the activities of these compounds in human cell lines and could be a valuable tool for structure based drug design of new selective $\alpha_4\beta_2$ nAChR ligands.

Conclusions

We have synthesized a new series of *N*-(arylalkyl)− and *N*-(aroylalkyl)-cytisines and found by binding studies on rat $\alpha_4\beta_2$ and α_7 receptor subtypes that a large number of them has a high affinity for $\alpha_4\beta_2$ subtype, with K_i values in the low nanomolar range for the best compounds and a rather poor affinity for α_7 subtype.

Three of these compounds (**3**, **27**, and **29**) have been tested previously, in heterologously expressed nicotinic subtypes, for their functional activity by using Ca^{2+} dynamic and electrophysiological recording.[14] All the three compounds showed antagonist/partial agonist activity toward the different subtypes, thus indicating that the N substituent greatly affect the efficacy of the cytisine derivatives. From these previous data, we expect that the new compounds can have antagonist/partial agonist activity, properties that have been explored for possible positive therapeutic effects.[1−5,36] However, the possibility that all or some of these compounds exhibit "receptor desensitizing" properties, as observed for the bulky 10-substituted cytisine derivatives described by Kozikowski et al.,[27d] deserves to be fully investigated.

The docking at the rat and human $\alpha_4\beta_2$ neuronal nicotinic receptor model permitted rationalization of the observed increasing potency produced by the presence in the ligand of a R terminal aromatic group (able to stack with Phe144) linked to the cytisine nitrogen by a short chain (two or three carbon atoms) bearing a group, like a carbonyl moiety, able to form hydrogen bonds. Further, the computational evaluation has evidenced that the potency of these compounds could be modulated by a larger number of hydrophobic interactions inside the binding site.

The applied flexible docking has shown a good correlation between the estimated free energy binding and the experimental binding data. Although the values of the correlation coefficients obtained for the docking scoring functions indicate a better fit for the rat $(\alpha_4)_2(\beta_2)_3$ model with respect to the human, as expected because the binding data were obtained on rat receptors, it is interesting to observe that these data are not very different from those obtained using human receptor model. These findings indicate that experimental binding data on rat cortex preparations are useful also to predict the binding affinity on human receptor subtypes.

Compounds **20**, **21**, **11**, **27**, **18**, **6**, and **25**, which are endowed with the highest affinity for $\alpha_4\beta_2$ receptor subtype (K_i in the range 2.6−35 nM), are characterized by a quite higher lipophilicity than cytisine and therefore more suitable for crossing the blood−brain barrier. Thus they deserve further investigations to define their in vivo pharmacological activities.

Finally, the present study may be useful to derive guidelines for the rational search of even more potent compounds.

Experimental Section

Chemistry. Melting points were taken in open glass capillaries on a Buchi apparatus and were uncorrected. ^{1}H NMR spectra were recorded in $CDCl_3$ or DMSO-d_6 on a Varian Gemini 200 spectrometer. Chemical shifts (δ) are reported in parts per million from the peak for internal Me_4Si. Values of the coupling constants (J) are reported in hertz. Cytisine protons are indicated as "α-pyr" or as "bisp" if pertinent, respectively, to the α-pyridone or to the bispidine moiety. Column chromatography (CC) was performed by using basic alumina (Across). Elemental analyses were performed on a Carlo Erba EA 1110 CHNS-O instruments in the Microanalysis Laboratory of the Department of Pharmaceutical Sciences of the University of Genoa. The analytical results are within ±0.3% of calculated values. The results of NMR spectra and elemental analyses indicated that the purity of all compounds was higher than 95%.

Intermediates. The required arylalkylhalides, ω-aroylalkylhalides, iodoacetamide, 2- and 4-vinylpyridine, acrylamide, methylvinylsulfone, 2-, 3-, and 4-hydroxymethylpyridine, and 3-(3-hydroxypropyl)pyridine were purchased from Aldrich. 3-(3-Bromopropyl)pyridine hydrobromide was prepared according to the method of Fabio et al.[37]

The 2-, 3-, and 4-bromomethylpyridines hydrobromides were prepared by the method of Bixler and Niemann.[38] The melting points corresponded to the literature.[39]

Preparation of Compounds 7, 8, 13, 14, 16−18, 20−22, and 28: General Method. In a Aldrich pressure tube, to a solution of cytisine (3−6 mmol) in MeCN (5−8 mL) the proper haloderivative (1.5−3 mmol) was added. The tube was flushed with N_2, closed, and heated to 100 °C for 20−24 h. A shorter time of heating (7 h) was sufficient for compound **18**, while compounds **13** and **17** required 36 h of heating. After cooling, the precipitate was filtered and the solution was concentrated to dryness. The residue was taken up in acidic H_2O, extracted with ether, and after alkalinization extracted with CH_2Cl_2. Compounds were purified as indicated in each case.

***N*-[2-(4-Fluorophenyl)ethyl]cytisine (7).** mp: 105−107 °C (Et_2O). Yield: 64%. ^{1}H NMR ($CDCl_3$) δ: 1.57−1.88 (m, 2H, bisp), 2.17−2.55 (m, 7H, 3H, bisp + 2H, N−CH_2 + 2H, CH_2−Ar), 2.73−2.94 (m, 3H, bisp), 3.79 (dd, 1H, J = 15.3, 5.9, bisp), 3.92 (d, 1H, J = 15.3, bisp), 5.88 (dd, 1H, J = 7, 1.3, α-pyr), 6.39 (dd, 1H, J = 9, 1.3, α-pyr), 6.67−6.90 (m, 4H, aromatic protons), 7.19 (dd, 1H, J = 9, 7, α-pyr). Anal. ($C_{19}H_{21}FN_2O$) C, H, N.

***N*-[2-(4-Methylphenyl)ethyl]cytisine (8).** mp: 139−140 °C (acetone). Yield: 72%. ^{1}H NMR ($CDCl_3$) δ: 1.58−1.91 (m, 2H, bisp), 2.12−2.54 (m, 10H, 3H, bisp + 2H, N−CH_2 + 2H, CH_2−Ar, superimposed on s at 2.21, 3H, CH_3), 2.74−2.98 (m, 3H, bisp), 3.81 (dd, 1H, J = 15.3, 5.9, bisp), 3.93 (d, 1H, J = 15.3, bisp), 5.90 (dd, 1H, J = 6.8, 1.2, α-pyr), 6.39 (dd, 1H, J = 9, 1.2, α-pyr), 6.74−7.02 (m, 4H, aromatic protons), 7.21 (dd, 1H, J = 9, 6.8, α-pyr). Anal. ($C_{20}H_{24}N_2O$) C, H, N.

***N*-[3-(4-Fluorophenyl)propyl]cytisine (13).** Oil °C (CC, Al_2O_3, CH_2Cl_2). Yield: 89%. ^{1}H NMR ($CDCl_3$) δ: 1.46−1.72 (m, 2H, CH_2-$\underline{CH_2}$-CH_2), 1.75−2.02 (m, 2H, bisp), 2.03−2.54 (m, 7H, 3H, bisp + 2H, N−CH_2 + 2H, CH_2−Ar), 2.78−3.10 (m, 3H, bisp), 3.92 (dd, 1H, J = 15.6, 7.6, bisp), 4.13 (d, 1H, J = 15.6, bisp), 6.03 (dd, 1H, J = 7.6, 1.6, α-pyr), 6.48 (dd, 1H, J = 8.8, 1.6, α-pyr), 6.82−6.89 (m, 4H, aromatic protons), 7.32 (dd, 1H, J = 8.8, 7.6, α-pyr).

The following are data for the hydrochloride. mp: 215−217 °C. Anal. ($C_{20}H_{23}FN_2O\cdot HCl$) C, H, N.

***N*-[3-(4-Methylphenyl)propyl]cytisine (14).** mp: 81−82 °C (Et_2O). Yield: 83%. ^{1}H NMR ($CDCl_3$) δ: 1.35−1.95 (m, 4H, 2H, bisp, + 2H, CH_2-$\underline{CH_2}$-CH_2), 1.98−2.45 (m, 10H, 3H bisp + 2H, N−CH_2 + 2H, CH_2−Ar, superimposed on s at 2.22, 3H, CH_3), 2.66−2.98 (m, 3H, bisp), 3.83 (dd, 1H, J = 15.7, 6.6, bisp), 4.02 (d, 1H, J = 15.7, bisp), 5.93 (dd, 1H, J = 6.8, 1.3, α-pyr), 6.38 (dd, 1H, J = 9, 1.3, α-pyr), 6.70−7.04 (m, 4H, aromatic protons), 7.23 (dd, 1H, J = 9, 6.8, α-pyr). Anal. ($C_{21}H_{26}N_2O$) C, H, N.

***N*-(4-Phenylbutyl)cytisine (16).** mp: 93−94 °C (Et_2O). Yield: 87%. ^{1}H NMR ($CDCl_3$) δ: 1.12−1.49 (m, 4H, CH_2-$\underline{CH_2}$-$\underline{CH_2}$-CH_2), 1.58−1.92 (m, 3H, bisp), 2.02−2.54 (m, 6H, 2H, bisp + 2H, N−CH_2 + 2H, CH_2−Ar), 2.68−2.97 (m, 3H, bisp), 3.81 (dd, 1H, J = 15.5, 6.2, bisp), 3.97 (d, 1H, J = 15.5, bisp), 5.89 (dd, 1H, J = 6.7, 1.3, α-pyr), 6.35 (dd, 1H, J = 9, 1.3, α-pyr), 6.89−7.35 (m, 6H, 5H, aromatic protons + 1H, α-pyr). Anal. ($C_{21}H_{26}N_2O$) C, H, N.

***N*-[4-(4-Fluorophenyl)butyl]cytisine (17).** mp: 95−96 °C (Et_2O). Yield: 52%. ^{1}H NMR ($CDCl_3$) δ: 1.12−1.43 (m, 4H, 2H, bisp, + 2H, CH_2-$\underline{CH_2}$-CH_2), 1.62−1.91 (m, 3H, bisp), 2.05−2.46 (m, 6H, 2H, bisp + 2H, N−CH_2 + 2H, CH_2−Ar), 2.67−2.94 (m, 3H, bisp), 3.81 (dd, 1H, J = 15.1, 6.7, bisp), 3.97 (d, 1H, J = 15.1, bisp), 5.88 (dd, 1H, J = 6.8, 1.3, α-pyr), 6.34 (dd, 1H, J = 9, 1.3, α-pyr), 6.77−7.02 (m, 4H, aromatic protons), 7.18 (dd, 1H, J = 9, 6.8, α-pyr). Anal. ($C_{21}H_{25}FN_2O$) C, H, N.

1-Phenyl-2-(cytisin-12-yl)-1-ethanone (18). mp: 138−140 °C (acetone) Yield: 82%. ^{1}H NMR ($CDCl_3$) δ: 1.72−1.97 (m, 2H, bisp), 2.37−2.48 (m, 1H, bisp), 2.53−2.70 (m, 2H, bisp), 2.75−3.00 (m. 3H, bisp), 3.44−3.63 (AB system, 2H, CH_2), 3.82 (dd, 1H, J = 15.4, 6.2, bisp), 3.91 (d, 1H, J = 15.4, bisp), 5.83 (dd, 1H, J = 7, 1.6, α-pyr), 6.37 (dd, 1H, J = 9.2, 1.6, α-pyr), 6.22−6.36 (m, 2H, aromatic protons), 6.41−6.54 (m, 1H, aromatic proton), 7.14 (dd, 1H, J = 9.2, 7.2, α-pyr), 7.72−7.83 (m, 2H, aromatic protons). Anal. ($C_{19}H_{20}N_2O_2$) C, H, N.

1-Phenyl-3-(cytisin-12-yl)-1-propanone (20). mp: 115−117 °C (Et_2O) Yield: 59%. ^{1}H NMR ($CDCl_3$) δ: 1.54−1.90 (m, 2H, bisp), 2.21−2.44 (m, 3H, bisp), 2.64 (t, 2H, J = 6.8, CH_2), 2.76−2.99 (m, 5H, 3H, bisp + 2H, CH_2), 3.80 (dd, 1H, J = 15.4, 6.4, bisp), 3.91 (d, 1H, J = 15.4, bisp), 5.88 (dd, 1H, J = 6.8, 1.3, α-pyr), 6.34 (dd, 1H, J = 9, 1.3, α-pyr), 7.18 (dd, 1H, J = 9, 6.8, α-pyr), 7.29−7.55 (m, 3H, aromatic protons), 7.71−7.82 (m, 2H, aromatic protons). Anal. ($C_{20}H_{22}N_2O_2$) C, H, N.

1-(4-Fluorophenyl)-3-(cytisin-12-yl)-1-propanone (21). Oil (CC, Al_2O_3, CH_2Cl_2). Yield: 75%. ^{1}H NMR ($CDCl_3$) δ: 1.55−1.92 (m, 2H, bisp), 2.16−2.41 (m, 3H, bisp), 2.61 (t, 2H, J = 6.7, $CH_2C(O)$), 2.72−2.98 (m, 5H, 3H, bisp + 2H, CH_2), 3.78 (dd, 1H, J = 15.1, 6.1, bisp), 3.90 (d, 1H, J = 15.1, bisp), 5.86 (dd, 1H, J = 6.8, 1.4, α-pyr), 6.33 (dd, 1H, J = 9, 1.4, α-pyr), 6.92−7.09 (m, 2H, aromatic protons), 7.17 (dd, 1H, J = 9, 6.8, α-pyr), 7.68−7.84 (m, 2H, aromatic protons).

The following data are for the hydrochloride. mp: 173−175 °C. Anal. ($C_{20}H_{21}FN_2O_2\cdot HCl\cdot 0.25H_2O$) C, H, N.

1-Phenyl-4-(cytisin-12-yl)-1-butanone (22). mp: 114−115 °C (acetone) Yield: 51%. ^{1}H NMR ($CDCl_3$) δ: 1.63−1.98 (m, 4H, 2H, bisp + 2H, CH_2-$\underline{CH_2}$-CH_2), 2.18−2.50 (m, 5H, 3H, bisp + 2H, CH_2), 2.68 (t, 2H, J = 7.6, $CH_2C(O)$), 2.80−2.99 (m, 3H, bisp), 3.87 (dd, 1H, J = 15.8, 6.4, bisp), 4.09 (d, 1H, J = 15.8, bisp), 5.92 (dd, 1H, J = 7, 1.6, α-pyr), 6.34 (dd, 1H, J = 9.2, 1.6, α-pyr), 7.14 (dd, 1H, J = 9.2, 7, α-pyr), 7.35−7.60 (m, 3H, aromatic protons), 7.72−7.84 (m, 2H, aromatic protons). Anal. ($C_{21}H_{24}N_2O_2$) C, H, N.

1-Methyl-4-(cytisin-12-yl)-1-butanone (28). mp: 94−96 °C (Et_2O) Yield: 27%. ^{1}H NMR ($CDCl_3$) δ: 1.37−1.58 (m, 2H, CH_2), 1.62−1.93 (m, 5H, 2H, bisp superimposed on s at 1.86 3H, CH_3), 1.99−2.42 (m, 7H, 3H, bisp + 2H, N−CH_2 + 2H, CH_2−C(O)), 2.65−2.94 (m, 3H, bisp), 3.78 (dd, 1H, J = 15.4, 6.5, bisp), 3.98 (dd, 1H, J = 15.4, bisp), 5.89 (dd, 1H, J = 7, 1.2, α-pyr), 6.36 (dd, 1H, J = 9, 1.2, α-pyr), 7.20 (dd, 1H, J = 9, 7, α-pyr). Anal. ($C_{16}H_{22}N_2O_2$) C, H, N.

Preparation of *N*-Pyridinylalkyl-cytisines 4, 5, 15: General Method. In a Aldrich pressure tube, to a solution of cytisine (0.57 g, 3 mmol) in MeCN (8 mL) the appropriate bromoalkylpyridine hydrobromide (1 mmol) was added. The tube was flushed with N_2, closed, and heated to 100 °C for 36 h. After cooling, the precipitate was filtered and the solution was concentrated to dryness. The residue was dissolved in acidic water, the acidic solution was extracted with ether and, after alkalinization, extracted with CH_2Cl_2. The organic phase was dried (Na_2SO_4), and the solvent was removed under vacuum; the residue was purified as indicated for each compound.

***N*-[(Pyridin-3-yl)methyl]cytisine (4).** mp: 128−129 °C (Et_2O). Yield: 64%. ^{1}H NMR ($CDCl_3$) δ: 1.64−1.96 (m, 2H, bisp), 2.19−2.48 (m, 3H, bisp), 2.66−2.97 (m, 3H, bisp), 3.23−3.51 (AB system, 2H, CH_2), 3.83 (dd, 1H, J = 16, 7.8, bisp), 4.05 (d, 1H, J = 16, bisp), 5.83 (dd, 1H, J = 7.4, 1.3, α-pyr), 6.42 (dd, 1H, J = 9.1, 1.3, α-pyr), 7.04 (dd, 1H, J = 9.1, 7.4, α-pyr), 7.14−7.30 (m, 2H, aromatic protons), 8.13−8.25 (m, 1H, aromatic proton), 8.31−8.42 (m, 1H, aromatic proton). Anal. ($C_{17}H_{19}N_3O$) C, H, N.

***N*-[(Pyridin-4-yl)methyl]cytisine (5).** mp: 121−122 °C (Et_2O). Yield: 57%. ^{1}H NMR ($CDCl_3$) δ: 1.58−1.94 (m, 2H, bisp), 2.14−2.45 (m, 3H, bisp), 2.53−2.95 (m, 3H, bisp), 3.13−3.47 (AB system, 2H, CH_2), 3.77 (dd, 1H, J = 15.4, bisp), 4.04 (d, 1H, J = 15.4, bisp), 5.81 (dd, 1H, J = 7.6, 1.4, α-pyr), 6.38 (dd, 1H, J = 9.2, 1.4, α-pyr), 6.64−6.88 (m, 2H, aromatic protons), 7.17 (dd, 1H, J = 9.2, 7.6, α-pyr), 8.14−8.38 (m, 2H, aromatic protons). Anal. ($C_{17}H_{19}N_3O$) C, H, N.

***N*-[3-(Pyridin-3-yl)propyl]cytisine (15).** Oil (CC, Al_2O_3, CH_2Cl_2). Yield: 45%. ^{1}H NMR ($CDCl_3$) δ: 1.24−1.78 (m, 4H, 2H bisp + 2H, $CH_2\underline{CH_2}CH_2$), 1.84−2.37 (m, 6H, 2H, bisp + 2H, N−CH_2 + 2H, CH_2−Ar), 2.54−2.89 (m, 3H, bisp), 3.08 (s, 1H, bisp), 3.72 (dd, 1H, J = 14.9, 5.8, bisp), 3.93 (d, 1H, J = 14.9, bisp), 5.88 (dd, 1H, J = 8, 1.2, α-pyr), 6.26 (dd, 1H, J = 8.8, 1.2, α-pyr), 6.82−7.08 (m, 2H, aromatic protons), 7.16 (dd, 1H, J = 8.8, 8, α-pyr), 7.92−8.04 (m, 1H, aromatic proton), 8.12−8.25 (m, 1H, aromatic proton).

The following data are for the hydrocloride. mp: 194−197 °C (d). Anal. ($C_{19}H_{23}N_3O \cdot HCl \cdot 1.75\ H_2O$) C, H, N.

(Cytisin-12-yl)acetamide (24). In an Aldrich pressure tube, to a solution of cytisine (0.57 g, 3 mmol) in MeCN (6 mL), iodoacetamide (0.56 g, 3 mmol) and anhydrous K_2CO_3 (0.41 g, 3 mmol) were added. The tube was flushed with N_2, closed, and heated at 100 °C for 7 h. After cooling, the precipitate was filtered and the solution was concentrated to dryness. The residue was taken up in acidic water, the acidic solution was extracted with ether and, after alkalinization, extracted with CH_2Cl_2. After drying (Na_2SO_4), the solution was concentrated to dryness and the residue crystallized from acetone. It is worth noting that this compound was previously isolated, as an oil from *Sophora exigua*.[40]

mp: 173−174 °C. Yield: 81%. ^{1}H NMR ($CDCl_3$) δ: 1.73−2.04 (m, 2H, bisp), 2.41−2.65 (m, 3H, bisp), 2.79−3.07 (m, 5H, 3H, bisp + 2H, CH_2), 3.88 (dd, 1H, J = 16, 6.8, bisp), 4.18 (d, 1H, J = 16, bisp), 5.24 (s, 1H, NH collapses with D_2O), 6.06 (s, 1H, NH collapses with D_2O, superimposed on dd at 6.02 dd, 1H, J = 6.9, 1.2, α-pyr), 6.45 (dd, 1H, J = 9.4, 1.2, α-pyr), 7.31 (dd, 1H, J = 9.4, 6.9, α-pyr). Anal. ($C_{13}H_{17}N_3O_2$) C, H, N.

Preparation of Compounds 10, 11, 25, and 26: General Method. Cytisine (0.38 g, 2 mmol) was dissolved in EtOH (10 mL) and treated with 2 mmol of the appropriate vinylcompound (2- and 4-vinylpyridine, acrylamide, methylvinylsulfone) and acetic acid (0.25 mL). The solution was refluxed for 24 h, under a stream of N_2, and afterwards was concentrated to dryness and taken up in acidic water. The acid solution was extracted with ether, made alkaline and extracted with CH_2Cl_2. The dichloromethane solution was dried (Na_2SO_4) and the solvent removed.

***N*-[2-(Pyridin-2-yl)ethyl]cytisine (10).** mp: 92−93 °C (Et_2O). Yield: 83%. ^{1}H NMR ($CDCl_3$) δ: 1.59−1.88 (m, 2H, bisp), 2.18−2.42 (m, 3H, bisp), 2.48−2.76 (m, 4H, 2H, N−CH_2 + 2H, CH_2−Ar), 2.78−2.95 (m, 3H, bisp), 3.64−3.85 (AB system, 2H, bisp), 5.85 (dd, 1H, J = 7, 1.4, α-pyr), 6.33 (dd, 1H, J = 9, 1.4, α-pyr), 6.66−6.78 (m, 1H, aromatic proton), 6.89−7.01 (m, 1H, aromatic proton), 7.16 (dd, 1H, J = 9, 7, α-pyr), 7.29−7.44 (m, 1H, aromatic proton), 8.28−8.38 (m, 1H, aromatic proton). Anal. ($C_{18}H_{21}N_3O$) C, H, N.

***N*-[2-(Pyridin-4-yl)ethyl]cytisine (11).** mp: 86−87 °C (Et_2O). Yield: 77%. ^{1}H NMR ($CDCl_3$) δ: 1.35−1.66 (m, 2H, bisp), 1.94−2.35 (m, 8H, 4H, bisp + 2H, N−CH_2 + 2H, CH_2−Ar), 2.49−2.72 (m, 2H, bisp), 3.52 (dd, 1H, J = 15.5, 6.3, bisp), 3.67 (d, 1H, J = 15.5, bisp), 5.67 (dd, 1H, J = 7.1, 1.5, α-pyr), 6.16 (dd, 1H, J = 9, 1.5, α-pyr), 6.46−6.65 (m, 2H, aromatic protons), 6.97 (dd, 1H, J = 9, 7.1, α-pyr), 7.95−8.16 (m, 2H, aromatic protons). Anal. ($C_{18}H_{21}N_3O$) C, H, N.

3-(Cytisin-12-yl)propionamide (25). mp: 185−187 °C (acetone). Yield: 71%. ^{1}H NMR ($CDCl_3$) δ: 1.74−1.99 (m, 2H, bisp), 2.09−2.61 (m, 7H, 3H, bisp + 2H, N−CH_2 + 2H, $CH_2C(O)$), 2.94−3.06 (m, 3H, bisp), 3.80 (dd, 1H, J = 15.3, 6.1, bisp), 4.07 (dd, 1H, J = 15.3, bisp), 4.82 (s, 1H, NH collapses with D_2O), 5.96 (dd, 1H, J = 7.1, 1.2, α-pyr), 6.36 (dd, 1H, J = 9.3, 1.2, α-pyr), 6.95 (s, 1H, NH collapses with D_2O), 7.23 (dd, 1H, J = 9.3, 7.1, α-pyr). Anal. ($C_{14}H_{19}N_3O_2$) C, H, N.

***N*-[2-(Methylsulfonyl)ethyl]cytisine (26).** mp: 83−84°C (Et_2O). Yield: 78% ^{1}H NMR ($CDCl_3$) δ: 1.58−1.97 (m, 2H, bisp), 2.21−2.58 (m, 8H, 3H, bisp + 2H, CH_2, superimposed on s at 2.39, 3H, CH_3), 2.62−3.08 (m, 5H, 3H, bisp + 2H, CH_2), 3.80 (dd, 1H, J = 15.5, 6, bisp), 3.96 (d, 1H, J = 15.5, bisp), 5.94 (dd, 1H, J = 6.8, 1.1, α-pyr), 6.34 (dd, 1H, J = 9.2, 1.1, α-pyr), 7.20 (dd, 1H, J = 9.2, 6.8, α-pyr). Anal. ($C_{14}H_{20}N_2O_3S$) C, H, N.

Binding Studies. Preparation of Tissue Sample. Cortex from 21 day old rats were dissected and immediately frozen . Frozen tissue was homogenized using a Potter homogenizer in an excess of buffer A (50 mM Tris-HCl pH 7, 120 mM NaCl, 5 mM KCl, 1 mM $MgCl_2$, 2.5 mM $CaCl_2$, and 2 mM phenylmethylsulfonyl fluoride), centrifuged (60 min at 30000*g*), and rinsed twice. The homogenates were resuspended in the same buffer containing 20 μg/mL of the protease inhibitors leupeptin, bestatin, pepstatin A, and aprotinin. Receptor expression ranged from 50 to 70 fmol/mg of protein.

[^{3}H]-Epibatidine Binding. (±)-[^{3}H]-epibatidine with a specific activity of 56−60 Ci/mmol was purchased from Perkin-Elmer (Boston MA); the nonradioactive α-bungarotoxin, nicotine, and epibatidine were purchased from Sigma. It has been previously reported that [^{3}H]-epibatidine also binds to α-bungarotoxin binding receptors with nM affinity.[41] To prevent the binding of [^{3}H]-epibatidine to the α-bungarotoxin binding receptors, the membrane homogenates were preincubated with 2 μM α-bungarotoxin and then with [^{3}H]-epibatidine. Preliminary time course experiments were performed before saturation and competition analyses to determine the time required for [^{3}H]-epibatidine to reach equilibrium with the $\alpha_4\beta_2$ nAChRs. In the epibatidine saturation experiments, aliquots of cortex homogenates were incubated overnight at 4 °C with concentrations of [^{3}H]-epibatidine ranging between 0.005 and 2.5 nM diluted in buffer A. Nonspecific binding was determined in parallel by means of incubation in the presence of 100 nM unlabeled epibatidine. At the end of the incubation, the samples were filtered on GFC filters presoaked in polyethylenimine through an harvester apparatus, and the filters were counted in a β counter. We determined a K_d value of [^{3}H]-epibatidine of 68 pM (CV = 15%). To test the ability of compounds to inhibit [^{3}H]-epibatidine binding, drugs were dissolved in water or DMSO and then diluted in buffer A just before use. The inhibition of radioligand binding by epibatidine, nicotine, cytisine and test compounds was measured by preincubated cortex homogenates with increasing doses (10 pM−10 mM) of the reference nicotinic agonists, epibatidine or nicotine, and the drug to be tested for 30 min at r.t., followed by overnight incubation with a final concentration of 0.005−0.1 nM [^{3}H]-epibatidine (concentration in the K_d range of [^{3}H]-epibatidine) at 4 °C.

[^{125}I]-α-Bungarotoxin Binding. [^{125}I]-α-Bungarotoxin with a specific activity of 200 Ci/mmol was purchased from Amersham. The saturation binding experiments were performed using aliquots of cortex membrane homogenates incubated overnight with 0.1−10 nM concentrations of [^{125}I]-α-bungarotoxin at rt. Nonspecific binding was determined in parallel by means of incubation in the presence of 1 μM unlabeled α-bungarotoxin. After incubation, the samples were filtered as described above and the bound radioactivity was directly counted in a γ counter. We determined a K_d value of [^{125}I]-α-bungarotoxin of 0.8 nM (CV = 25%).The inhibition of radioligand binding by epibatidine, nicotine, and the test compounds was measured by preincubating cortex homogenates with increasing doses (10 pM−10 mM) of the reference nicotinic agonists, epibatidine or nicotine, and the drug to be tested for 30 min at rt, followed by overnight incubation with a final concentration of 1 nM [^{125}I]-α-bungarotoxin (concentration in the K_d range of [^{125}I]-α-bungarotoxin) at the same temperatures as those used for the saturation experiments.

Data Analysis. For each compound, the experimental data obtained from the three saturation and three competition binding experiments were analyzed by means of a nonlinear least-squares procedure using the LIGAND program as described by Munson and Rodbard.[42] The binding parameters were calculated by simultaneously fitting three independent saturation experiments, and the K_i values were determined by fitting the data of three independent competition experiments. The errors in the K_D and K_i values of the simultaneous fits were calculated using the LIGAND software and were expressed as percentage coefficients of variation (% CV). When final compound concentrations up to 200 μM did not inhibit radioligand binding, the K_i value was defined as being > 100 μM based on the Cheng and Prusoff's equation.

Molecular Modeling. The three-dimensional structure of the 29 examined ligands in their protonated forms were built and

energy minimized within Ghemical[43] starting from the X-ray structure of **20**.[34] All calculations were performed on a 3.0 GHz Quad-Xeon 64-bit workstation running under the CentOS4.4 x86_64 Linux distribution. The Fortran software sources for "Modeler" and "Tinker" were recompiled using the 64-bit optimizations to suit the 64-bit and SMP CPU architecture.

Molecular Docking. The rat and human $\alpha_4\beta_2$ models were used for docking studies with the program AutoDock (version 4.0).[44] First, it was checked if AutoDock was able to find the correct position of the cocrystallized ligand (*Aplysia californica* AChBP cocrystallized with epibatidine, PDP code: 2BYQ). The docking software was able to detect the conformation of epibatidine molecule within the 10 best docking poses with an rmsd value below 1.5 Å. The cytisine derivatives (**1**−**29**) were docked at the putative binding site by using a two-step docking process. The docking procedure was at first applied to the whole protein target, without imposing any binding site, using the so-called "blind docking" approach.[45] A grid map was generated for the whole protein target, centered at the middle of the receptor models and using a grid resolution of 0.55 Å. The resulting docked conformations were clustered into families of similar binding modes, with a root-mean-square deviation (rmsd) clustering tolerance of 2 Å. In almost all cases, the lowest docking-energy conformations were included in the largest cluster found (which usually contains 80−100% of total conformations), then the lowest docking-energy conformations were considered as the most stable orientations. Second, we docked the ligands in the identified binding site ("refined docking"): a radius of 7 Å centered on the best-scored conformation previously obtained was considered, with a finer grid resolution (∼0.36 Å). The resulting orientations were again clustered, considering a root-mean-square deviation (rmsd) tolerance of 2.0 Å, into families, and the lowest docking-energy conformations were then equilibrated for 1.2 ns by unrestrained MD. The simulations were performed at constant temperature and pressure (NPT ensemble) in a periodic cubic box of TIP3P water molecules. The water bond distances and angle forced using the SETTLE algorithm,[46] while the bond lengths within the protein were constrained with the LINCS algorithm.[47] The coupling time was set to 1.0 ps, and the isothermal compressibility was set to 4.6×10^{-5} bar^{-1}. The protein, ligand, and solvent were independently coupled to a temperature of 298 K, coupling time 0.1 ps, and the pressure was held at 1 bar, coupling time 0.2 ps, using a Berendsen thermostat to maintain temperature and pressure unvarying. The time step used was 1.0 fs. Snapshots of the receptor−substrate system were saved every 0.2 ps. Finally a total of 6000 snapshots were saved. Hydrogen bonds and contacts were automatically identified using contact module of CCP4,[48] while the other interactions were identified visually.

Hybrid QM/MM Calculations. In the current study, we used the pseudobond ab initio QM/MM approach, as implemented in Gaussian03.[49] This methodology circumvents the major deficiency of the conventional link-atom QM/MM approach, providing a consistent and well-defined ab initio QM/MM potential energy surface. For the QM/MM calculations, the receptor−ligand systems resulting from the docking study were first partitioned into a QM subsystem and then in an MM subsystem. The reaction system used a smaller QM subsystem, formed by the ligand and amino acid side chains within 3.5 Å from the ligand, while the rest of the protein (the MM subsystem) was treated using the AMBER force field. together with a low memory convergence algorithm. The boundary problem between the QM and MM subsystems was solved using the pseudobond approach. With this receptor−substrate QM/MM system, an iterative optimization procedure was applied to the QM/MM system, using a B3LYP/3-21G* QM/MM calculation, leading to an optimized structure for the reactants. The convergence criterion used was set to obtain an energy gradient less than 10^{-4} using the twin-range cutoff method for nonbonded interactions, with a long-range cutoff of 14 Å and a short-range cutoff of 8 Å.

Acknowledgment. Financial support from MIUR (Ministero dell'Istruzione, dell'Università e della Ricerca, Rome, Italy) is gratefully acknowledged.

Supporting Information Available: Binding affinity (K_i, nM) of some cytisine derivatives to rat cortex $\alpha_4\beta_2$ receptor subtype labeled with [^{3}H]-epibatidine and [^{3}H]-cytisine respectively; amino acid content of the rat and human binding pockets within 5 Å radius; amino acids involved in the cytisine binding; elemental analysis results for the novel N-substituted cytisine derivatives. This material is available free of charge via the Internet at http://pubs.acs.org.

References

(1) (a) Gotti, C.; Fornasari, D.; Clementi, F. Human neuronal nicotinic acetylcholine receptors. *Prog. Neurobiol.* **1997**, *53*, 199–237. (b) Gotti, C.; Zoli, M.; Clementi, F. Brain nicotinic acetylcholine receptors: native subtypes and their relevance. *Trends Pharmacol. Sci.* **2006**, *27*, 482–491.

(2) Holladay, M. W.; Dart, M. J.; Lynch, J. K. Neuronal nicotinic acetylcholine receptors as targets for drug discovery. *J. Med. Chem.* **1997**, *40*, 4169–4194.

(3) Gotti, C.; Clementi, F. Neuronal nicotinic receptors: from structure to pathology. *Prog. Neurobiol.* **2004**, *74*, 363–396.

(4) Cassels, B. K.; Bermúdez, I.; Dajas, F.; Abin-Carriquiry, J. A.; Wonnacott, S. From ligand design to therapeutic efficacy: the challenge for nicotinic receptor research. *Drug Discovery Today* **2005**, *10*, 1657–1665.

(5) Jensen, A. A.; Frolund, B.; Liljefors, T.; Krogsgaard-Larsen, P. Neuronal nicotinic acetylcholine receptors: structural revelations, target identifications, and terapheutic inspirations. *J. Med. Chem.* **2005**, *48*, 4705–4745.

(6) Lin, N.-H.; Meyer, M. D. Recent developments in neuronal nicotinic acetylcholine receptor modulators. *Expert Opin. Ther. Patents* **1998**, *8*, 991–1015.

(7) Bunnelle, W. H.; Dart, M. J.; Schrimpf, M. R. Design of ligands for the nicotinic acetylcholine receptors: the quest for selectivity. *Curr. Top. Med. Chem.* **2004**, *4*, 299–334.

(8) Glennon, R. A. Medicinal Chemistry of $\alpha 4\beta 2$ nicotinic cholinergic receptor ligands. *Prog. Med. Chem.* **2004**, *42*, 55–123.

(9) (a) Holladay, M. W.; Wasicak, J. T.; Lin, N. H.; Ne, Y.; Ryther, K. B.; Bannon, A. W.; Buckley, M. J.; Kim, D. J.; Decker, M. W.; Anderson, D. J.; Campbell, J. E.; Kuntzweiler, T. A.; Donnelly-Roberts, D. L.; Piattoni-Kaplan, M.; Briggs, C. A.; Williams, M.; Arneric, S. D. Identification and initial structure−activity relationships of (*R*)-5-(2-azetidinylmethoxy)-2-chloropyridine (ABT-594), a potent, orally active, non-opiate analgesic agent acting via neuronal nicotinic acetylcholine receptors. *J. Med. Chem.* **1998**, *41*, 407–412. (b) Bannon, A. W.; Decker, M. W.; Holladay, M. W.; Curzon, P.; Donnelly-Roberts, D.; Puttfarcken, P. S.; Bitner, R. S.; Diaz, A.; Dickenson, A. H.; Porsolt, R. D.; Williams, M.; Arneric, S. P. Broad spectrum, non-opioid analgesic activity by selective modulation of neuronal nicotinic acetylcholine receptors. *Science* **1998**, *279*, 77–81.

(10) (a) Arneric, S. P.; Sullivan, J. P.; Briggs, C. A.; Donnelly-Roberts, O.; Anderson, D. J.; Raszkiewicz, J. L.; Hughes, M. L.; Cadman, E. D.; Adams, P.; Garvey, D. S. (S)-3-Methyl-5-(1-methyl-2-pyrrolidinyl)isoxazole (ABT-418): a novel cholinergic ligand with cognition-enhancing and anxiolytic activities: I. In vitro characterization. *J. Pharmacol. Exp. Ther.* **1994**, *270*, 310–318. (b) Decker, M. W.; Brioni, J. D.; Sullivan, J. P.; Buckley, M. J.; Radek, R. J.; Raszkiewicz, J. L.; Kang, C. H.; Kim, D. J.; Giardina, W. J.; Wasicak, J. T. (S)-3-Methyl-5-(1-methyl-2-pyrrolidinyl)isoxazole (ABT-418): a novel cholinergic ligand with cognition-enhancing and anxiolytic activities: II. In vivo characterization. *J. Pharmacol. Exp. Ther.* **1994**, *270*, 319–328.

(11) (a) Bourn, W. M.; Keller, W. J.; Bonfiglio, J. F. Comparison of mescal bean alkaloids with mescaline, Δ^9-THC and other psychotogens. *Life Sci.* **1979**, *25*, 1043–1054. (b) El-Seedi, H. R.; De Smet, P. A. G. M.; Beck, O.; Possnert, G.; Bruhn, J. G. *J. Ethnopharmacol.* **2005**, *101*, 238–242.

(12) (a) Wonnacott, S. Brain nicotine binding sites. *Hum. Toxicol.* **1987**, *6*, 343–353. (b) Pabreza, L. A.; Dhawan, S.; Kellar, K. J. [^{3}H]-Cytisine binding to nicotine cholinergic receptors in brain. *Mol. Pharmacol.* **1991**, *39*, 9–12. (c) Hall, M.; Zerbe, L.; Leonard, S.; Freedman, R. Characterization of [^{3}H]cytisine binding to human brain membrane preparations. *Brain Res.* **1993**, *600*, 127–133.

(13) (a) Papke, R. L.; Heinemann, S. F. Partial agonist properties of cytisine on neuronal nicotinic receptors containing the beta 2 subunit. *Mol. Pharmacol.* **1994**, *45*, 142–149. (b) Chavez-Noriega, L. E.; Crona, J. H.; Washburn, M. S.; Urrutia, A.; Elliott, K. J.; Johnson, E. C. Pharmacological characterization of recombinant human and neuronal nicotinic acetylcholine receptors h$\alpha_2\beta_2$, h$\alpha_2\beta_4$, h$\alpha_3\beta_2$, h$\alpha_3\beta_4$, h$\alpha_4\beta_2$, h$\alpha_4\beta_3$, andα_7 expressed in Xenopus oocytes. *J. Pharmacol. Exp. Ther.* **1997**, *280*, 346–356. (c) Xiao, Y.; Kellar, K. J. The comparative pharmacology and up-regulation of rat neuronal nicotinic receptor subtype binding sites stably expressed in transfected mammaliam cells. *J. Pharmacol. Exp. Ther.* **2004**, *310*, 98–107.

(14) Carbonnelle, E.; Sparatore, F.; Canu Boido, C.; Salvagno, C.; Baldani Guerra, B.; Terstappen, G.; Zwart, R.; Vijverberg, H.; Clementi, F.; Gotti, C. Nitrogen substitution modifies the activity of cytisine on neuronal nicotinic receptor subtypes. *Eur. J. Pharmacol.* **2003**, *471*, 85–96.

(15) (a) Barlow, R. B.; McLeod, L. J. Some studies on cytisine and its methylated derivatives. *Br. J. Pharmacol.* **1969**, *35*, 161–174. (b) Sloan, J. W.; Martin, W. R.; Bostwik, M.; Hook, R.; Wala, E. The comparative binding characteristics of nicotinic ligands and their pharmacology. *Pharmacol., Biochem. Behav.* **1988**, *30*, 255–267. (c) Museo, E.; Wise, R. A. Cytisine induced behavioural activation: delineation of neuroanatomical locus of action. *Brain Res.* **1995**, *670*, 257–263. (d) Rao, T. S.; Correa, L. D.; Reid, R. T.; Lloyd, G. K. Evaluation of antinociceptive effects of neuronal nicotinic acetylcholine receptors ligands in rat tail-flick assay. *Neuropharmacology* **1996**, *35*, 393–405. (e) Seale, T. W.; Singh, R. S.; Basmadjian, G. Inherited selective hypoanalgesic response to cytisine in the tail-flick test in CF-1 mice. *NeuroReport* **1998**, *9*, 201–205. (f) Ferger, B.; Spratt, C.; Teismann, P.; Seitz, K.; Kuschinsky, K. Effects of cytisine on hydroxyl radicals in vitro and MPTP-induced dopamine depletion in vivo. *Eur. J. Pharmacol.* **1998**, *360*, 155–163.

(16) (a) Dallemagne, M. G.: Heymans, C. H. Respiratory stimulants. In Manske, R. H. F. Ed.; The Alkaloids, vol. 5; Academic Press: New York, 1955; pp 109−139. (b) Zakusov, V. V. Farmacologiia, Medgiz: Moscow, 1960, p 203.

(17) (a) Paun, D.; Franze, J. Raucherentwohnung mit cytisinhaltigen "Tabex" Tabletten. *Dtsch. Gesundheitswes.* **1968**, *23*, 2088–2091. (b) Benndorf, S.; Kempe, G.; Scharfenberg, G.; Wendekamm, R.; Winkelvoss, E. Ergebnisse der medikamentosen Raucherentwohnung mit Cytisin (Tabex). *Dtsch. Gesundheitswes.* **1968**, *23*, 2092–2096. (c) Seeger, R. Cytisin als Raucherentwohnungmittel? *Med. Monatschr. Pharm.* **1992**, *15*, 20–21. (d) Etter, J.-F. Cytisine for smoking cessation. A literature review and a meta-analysis. *Arch Intern. Med.* **2006**, *166*, 1553–1559. (e) Etter, J.-F.; Lukas, R. J.; Benowitz, N. L.; West, R.; Dresler, C. M. Cytisine for smoking cessation: A research agenda. *Drug Alcohol Dep.* **2008**, *92*, 3–8.

(18) (a) Murakoshi, I.; Fuji, Y.; Takedo, S.; Arai, J. Lupin alkaloids as antidiabetics. Jpn. Kokai Tokkyo Koho, Japanese Patent 04-295480, **1992**; *Chem Abstr.* **1993**, *118*, 45733. (b) Murakoshi, I.; Fuji, Y.; Kawamura, H.; Marayama, H. Lupine alkaloids as antiinflammatory agents. Jpn. Kokai Tokkyo Koho, Japanese Patent 04-295479 (1992); *Chem Abstr.* **1993**, *118*, 45734

(19) Lippiello, P. M.; Cladwell, W. S. Neurodegenerative diseases treatment with cytisine compounds (*RJ Reynolds Tobacco Co.*). U.S. Patent US 5,242,916, **1993**; *Chem. Abstr.* **1993**, *119*, 217429

(20) O'Neill, B. T. Preparation of pyridone-fused azabicyclic- or cytisine derivatives for use in addiction therapy. Patent PCT Int. Appl. WO98 1998, 18, 798, **1998**; *Chem. Abstr.* **1998**, *129*, 4774

(21) (a) Canu, C.; Sparatore, F. Cytisine derivatives as ligands for nicotinic receptor subtypes. Ital. Hung. Polish Joint Meet. on Med. Chem., Giardini Naxos, Sept 28−Oct 1, 1999. Abstracts book p 206. (b) Canu Boido, C.; Sparatore, F. Synthesis and preliminary pharmacological evaluation of some cytisine derivatives. *Farmaco* **1999**, *54*, 438–451.

(22) Nicolotti, O.; Canu Boido, C.; Sparatore, F.; Carotti, A. Cytisine derivatives as high affinity nAChR ligands: synthesis and comparative molecular field analysis. *Farmaco* **2002**, *57*, 469–478.

(23) Canu Boido, C.; Tasso, B.; Boido, V.; Sparatore, F. Cytisine derivatives as ligands for neuronal nicotinic receptors and with various pharmacological activities. *Farmaco* **2003**, *58*, 265–277.

(24) Riganti, L.; Matteoni, C.; Di Angelantonio, S.; Nistri, A.; Gaimarri, A.; Sparatore, F.; Canu Boido, C.; Clementi, F.; Gotti, C. Long-term exposure to the new nicotinic antagonist 1,2-bis-*N*-cytisinylethane upregulates nicotinic receptor subtypes of SH-SY5Y human neuroblastoma cells. *Br. J. Pharmacol.* **2005**, *146*, 1096–1109.

(25) (a) Imming, P.; Klaperski, P.; Stubbs, M. T.; Seitz, G.; Gundisch, D. Syntheses and evaluation of halogenated cytisine derivatives and of bioisosteric thiocytisine as potent and selective nAChR ligands. *Eur. J. Med. Chem.* **2001**, *36*, 375–388. (b) Fitch, R. W.; Kaneko, Y.; Klaperski, P.; Daly, J. W.; Seitz, G.; Gundisch, D. Halogenated and isosteric cytisine derivatives with increased affinity and functional activity at nicotinic acetylcholine receptors. *Bioorg. Med. Chem. Lett.* **2005**, *15*, 1221–1224.

(26) (a) Houlihan, L. M.; Slater, Y.; Guerra, D. L.; Peng, J.-H.; Kuo, Y.-P.; Lukas, R. J.; Cassels, B. K.; Bermúdez, I. Activity of cytisine and its brominated isosteres on recombinant human α_7, $\alpha_4\beta_2$, and $\alpha_4\beta_4$ nicotinic acetylcholine receptors. *J. Neurochem.* **2001**, *78*, 1029–1043. (b) Slater, Y. E.; Houlihan, L. M.; Maskell, P. D.; Exley, R.; Bermúdez, I.; Lukas, R. J.; Valdivia, A. C.; Cassels, B. K. Halogenated cytisine derivatives as agonists at human neuronal nicotinic acetylcholine receptor subtypes. *Neuropharmacology* **2003**, *44*, 503–515. (c) Abin-Carriquiry, J. A.; Voutilainen, M. H.; Barik, J.; Cassels, B. K.; Iturriaga-Vásquez, P.; Bermúdez, I.; Durand, C.; Dajas, F.; Wonnacott, S. C3-halogenation of cytisine generates potent and efficacious nicotinic receptor agonists. *Eur. J. Pharmacol.* **2006**, *536*, 1–11. (d) Abin-Carriquiry, J. A.; Costa, G.; Urbanavicius, J.; Cassels, B. K.; Rebolledo-Fuentes, M.; Wonnacott, S.; Dojes, F. In vivo modulation of dopaminergic nigrostriatal pathways by cytisine derivatives: Implications for Parkinson's Disease. *Eur. J. Pharmacol.* **2008**, *589*, 80–84.

(27) (a) Marrière, E.; Rouden, J.; Tadino, V.; Lasne, M.-C. Synthesis of analogues of (−)-cytisine for in vivo studies of nicotinic receptors using positron emission tomography. *Org. Lett.* **2000**, *2*, 1121–1124. (b) Roger, G.; Lagnel, B.; Rouden, J.; Besret, L.; Valette, H.; Demphel, S.; Gopisetti, J. M.; Coulon, C.; Ottaviani, M.; Wrenn, L. A.; Letchworth, S. R.; Bohme, G. A.; Benavides, J.; Lasne, M.-C.; Bottlaender, M.; Dollé, F. Synthesis of a [2-pyridinyl-^{18}F]-labelled fluoro derivative of (−)-cytisine as a candidate radioligand for brain nicotinic $\alpha_4\beta_2$ receptor imaging with PET. *Bioorg. Med. Chem.* **2003**, *11*, 5333–5343. (c) Chellappan, S. K.; Xiao, Y.; Tueckmontel, W.; Kellar, K. J.; Kozikowski, A. P. Synthesis and pharmacological evaluation of novel 9- and 10-substituted cytisine derivatives. Nicotinic ligands of enhanced subtype selectivity. *J. Med. Chem.* **2006**, *49*, 2673–2676. (d) Kozikowski, A. P.; Chellapan, S. K.; Xiao, Y.; Bajjuri, K. M.; Yuan, H.; Kellar, K. J.; Petukhov, P. A. Chemical medicine: novel 10-substituted cytisine derivatives with increased selectivity for $\alpha_4\beta_2$ nicotinic acetylcholine receptors. *ChemMedChem* **2007**, *2*, 1157–1161.

(28) (a) Rouden, J.; Ragot, A.; Gouault, S.; Cahard, D.; Plaquevent, J.-C.; Lasne, M.-C. Regio- and diastereoselective functionalization of (−)-cytisine: an unusual N-C acyl migration. *Tetrahedron: Asymmetry* **2002**, *13*, 1299–1305. (b) Houllier, N.; Gouault, S.; Lasne, M.-C.; Rouden, J. Regio and diastereoselective functionalization of (−)-cytisine. *Tetrahedron* **2006**, *62*, 11679–11686.

(29) (a) Kozikowski, A. P.; Musachio, J. L.; Kellar, K. J.; Xiao,Y.; Wei, Z.-L. Ligands for nicotinic acetylcholine receptors, and methods of making and using them. Patent PCT WO2005/000806 A2, 2005. (b) Tilotta, M. C. *Novel nicotinic acetylcholine receptor ligands based on cytisine, ferruginine, anatoxin-a and choline: in vitro evaluation and structure-activity relationships*. http://hss.ulb.unibonn.de/diss_online/math_nat_fak/2004/tilotta_maria/0464.pdf.December2, 2005.

(30) (a) Rakhimov, Sh.B.; Vinogradova, V. J.; Mirzaev, Y. R.; Vyrova, N. L.; Kuzantseva, D. S. Synthesis and biological activity of *N*-benzyl derivatives of cytisine. *Chem. Nat. Compd.* **2006**, *42*, 462–469. (b) Safrykine, V. A.; Vinogradova, V. J.; Ambartsumova, R. F.; Ibragimov, T. F.; Shakhidoyatov, K. M. Thiazole and benzothiazole derivatives of cytisine. *Chem. Nat. Compd.* **2006**, *42*, 470–472. (c) Frasinyak, M. S.; Turov, A. V.; Vinogradova, V. I.; Khilya, V. P. Aminomethylation of cytisine by 3-hetaryl-7-hydroxychromones. *Chem. Nat. Compd.* **2007**, *43*, 285–290. (d) Nizri, E.; Irony-Tur-Sinai, M.; Lavon, I.; Meshulam, H.; Amitai, G.; Brenner, T. IBU-Octyl-cytisine, a novel bifunctional compound eliciting anti-inflammatory and cholinergic activity, ameliorates CNS inflammation by inhibition of T-cell activity. *Int. Immunopharm.* **2007**, *7*, 1129–1139.

(31) (a) Coe, J. W.; Brooks, P. R.; Vetelino, M. G.; Wirtz, M. C.; Arnold, E. P.; Huang, J.; Sands, S. B.; Davis, T. I.; Lebel, L. A.; Fox, C. B.; Shrikhande, A.; Heym, J. H.; Schaeffer, E.; Rollema, H.; Lu, Y.; Mansbach, R. S.; Chambers, L. K.; Rovetti, C. C.; Schulz, D. W.; Tingley, F. D.; O'Neill, B. T. Varenicline, an $\alpha_4\beta_2$ nicotinic receptor partial agonist for smoking cessation. *J. Med. Chem.* **2005**, *48*, 3474–3477. (b) Coe, J. W.; Vetelino, M. G.; Bashore, C. G.; Wirtz, M. C.; Brooks, P. R.; Arnold, E. P.; Lebel, L. A.; Fox, C. B.; Sands, S. B.; Davis, T. I.; Schulz, D. W.; Rollema, H.; Tingley, F. D.; O'Neill, B. T. In pursuit of $\alpha_4\beta_2$ nicotinic partial agonists for smoking cessation: carbon analogs of (−)-cytisine. *Bioorg. Med. Chem. Lett.* **2005**, *15*, 2974–2979. (c) Coe, J. W.; Brooks, P. R.; Wirtz, M. C.; Bashore, C. G.; Bianco, K. E.; Vetelino, M. G.; Arnold, E. P.; Lebel, L. A.; Fox, C. B.; Tingley, F. D.; Schulz, D. W.; Davis, T. I.; Sands, S. B.; Mansbach, R. S.; Rollema, H.; O'Neill, B. T. 3,5-Bicyclic arylpiperidines: a novel class of $\alpha_4\beta_2$ neuronal nicotinic receptor partial agonists for smoking cessation. *Bioorg. Med. Chem. Lett.* **2005**, *15*,

4889–4897. (d) Steensland, P.; Simms, J. A.; Holgate, J.; Richards, J. K.; Bartlett, S. E. Varenicline, as $\alpha_4\beta_2$ nicotinic acetylcholine receptor partial agonist, selectively decreases ethanol consumption and seeking. *Proc. Natl. Acad. Sci. U.S.A.* **2007**, *104*, 12518–12523. (e) Eisenberg, M. J.; Filion, K. B.; Yavin, D.; Bélisle, P.; Mottillo, S.; Joseph, B.; Gervais, A.; O'Loughlin, J.; Paradis, G.; Rinfret, S.; Pilote, L. Pharmacotherapies for smoking cessation: a meta-analysis of randomized controlled trials. *CMAY* **2008**, *179*, 135–144.

(32) (a) Brejc, K.; van Dijk, W. J.; Klaassen, R. V.; Schuurmans, M.; van der Oost, J.; Smit, A. B.; Sixma, T. K. Crystal structure of an ACh-binding protein reveals the ligand-binding domain of nicotinic receptors. *Nature* **2001**, *411*, 269–276. (b) Unwin, N. Refined structure of the nicotinic acetylcholine receptor at 4 Å resolution. *J. Mol. Biol.* **2005**, *346*, 967–989. (c) Le Novère, N.; Grutter, T.; Changeux, J.-P. Models of the extracellular domain of nicotinic receptors and of agonist and Ca^{+2} binding sites. *Proc. Natl. Acad. Sci. U.S. A.* **2002**, *99*, 3210–3215.

(33) Bourne, Y.; Talley, T. T.; Hansen, S. B.; Taylor, P.; Marchot, P. Crystal structure of a Cbtx-AchBP complex reveals essential interactions between snake alpha-neurotoxins and nicotinic receptors. *EMBO J.* **2005**, *24*, 1512–1522.

(34) Bombieri, G.; Meneghetti, F.; Artali, R.; Tasso, B.; Canu Boido, C.; Sparatore, F. The influence of the nitrogen substitution in three cytisine derivatives as ligands for the neuronal nAChRs: a structural and theoretical study. *Chem. Biodiversity* **2008**, *5*, 1867–1878.

(35) Artali, R.; Bombieri, G.; Meneghetti, F. Docking of 6-chloropyridazin-3-yl derivatives active on nicotinic acetylcholine receptors into molluscan acetylcholine binding protein (AChBP). *Farmaco* **2005**, *60*, 313–320.

(36) (a) Dwoskin, L. P.; Xu, R.; Ayers, J. T.; Crooks, P. A. Recent developments in neuronal nicotinic acetylcholine receptor antagonists. *Expert Opin. Ther. Patents* **2000**, *10*, 1561–1581. (b) Dwoskin, L. P.; Crooks, P. A. Competitive neuronal nicotinic receptor antagonists: a new direction for drug discovery. *J. Pharmacol. Exp. Ther.* **2001**, *298*, 395–402.

(37) Fabio, P. F.; Lang, S. A.; Lin, Y.-I; Tomcufcik, A. S. Antiamebic amidines and sulfonamides of 5- and 6-amino-2,3-bis(4-alkyl-1-piperazinyl)quinoxalines. *J. Med. Chem.* **1980**, *23*, 201–206.

(38) Bixler, L. B.; Nieman, C. Synthesis of b-(4-pyridyl)-DL-alanine and of b-(4-pyridyl-1-oxide)-DL, D- and L-alanine. *J. Org. Chem.* **1958**, *23*, 575–584.

(39) Coombes, R. G.; Johnson, H. D.; Winterton, N. s-Bonded organotransition-metal ions. Part I. The formation of air-stable pentaaquopyridiomethylchromium (III) ions. *J. Chem. Soc.* **1965**, 7029–7035.

(40) Takamatsu, S; Saito, K; Ohmiya, S.; Ruangrangsi, N.; Murakoshi, I. Lupin alkaloids from Sophora exigua. *Phytochemistry* **1991**, *30*, 3793–3795.

(41) Balestra, B.; Moretti, M.; Longhi, R.; Mantegazza, R.; Clementi, F.; Gotti, C. Antibodies against neuronal nicotinic receptor subtypes in neurological disorders. *J. Neuroimmunol.* **2000**, *102*, 89–97.

(42) Munson, P. J.; Rodbard, D. LIGAND: a versatile computerized approach for characterization of ligand-binding systems. *Anal. Biochem.* **1980**, *107*, 220–239.

(43) Ghemical molecular modelling package. [http://www.bioinformatics.org/ghemical.

(44) (a) Morris, G. M.; Goodsell, D. S.; Halliday, R. S.; Huey, R.; Hart, W. E.; Belew, R. K.; Olson, A. J. Automated Docking Using a Lamarckian Genetic Algorithm and Empirical Binding Free Energy Function. *J. Comput. Chem.* **1998**, *19*, 1639–1662. (b) Huey, R.; Morris, G. M.; Olson, A. J.; Goodsell, D. S. A Semiempirical Free Energy Force Field with Charge-Based Desolvation. *J. Comput. Chem.* **2007**, *28*, 1145–1152.

(45) (a) Hetényi, C.; van der Spoel, D. Efficient docking of peptides to proteins without prior knowledge of the binding site. *Protein Sci.* **2002**, *11*, 1729–1737. (b) Hetényi, C.; van der Spoel, D. Blind docking of drug-sized compounds to proteins with up to a thousand residues. *FEBS Lett.* **2006**, *580*, 1447–1450.

(46) Miyamoto, S.; Kollman, P. A. SETTLE—an analytical version of the shake and rattle algorithm for rigid water models. *J. Comput. Chem.* **1992**, *13*, 952–962.

(47) Hess, B.; Bekker, H.; Berendsen, H. J. C.; Fraaije, J. G. E. M. LINCS: a linear constraint solver for molecular simulations, *J. Comput. Chem.*, **1997**, *18*, 1463−1472.

(48) Collaborative Computational Project, Number 4. The CCP4 Suite: Programs for Protein Crystallography. *Acta Crystallogr., Sect. D: Biol Crystallogr.* **1994**, *50*, 760−763.

(49) Frisch, M. J.; Trucks, G. W.; Schlegel, H. B.; Scuseria, G. E.; Robb, M. A.; Cheeseman, J. R.; Montgomery, J. A., Jr.; Vreven, T.; Kudin, K. N.; Burant, J. C.; Millam, J. M.; Iyengar, S. S.; Tomasi, J.; Barone, V.; Mennucci, B.; Cossi, M.; Scalmani, G.; Rega, N.; Petersson, G. A.; Nakatsuji, H.; Hada, M.; Ehara, M.; Toyota, K.; Fukuda, R.; Hasegawa, J.; Ishida, M.; Nakajima, T.; Honda, Y.; Kitao, O.; Nakai, H.; Klene, M.; Li, X.; Knox, J. E.; Hratchian, H. P.; Cross, J. B.; Bakken, V.; Adamo, C.; Jaramillo, J.; Gomperts, R.; Stratmann, R. E.; Yazyev, O.; Austin, A. J.; Cammi, R.; Pomelli, C.; Ochterski, J. W.; Ayala, P. Y.; Morokuma, K.; Voth, G. A.; Salvador, P.; Dannenberg, J. J.; Zakrzewski, V. G.; Dapprich, S.; Daniels, A. D.; Strain, M. C.; Farkas, O.; Malick, D. K.; Rabuck, A. D.; Raghavachari, K.; Foresman, J. B.; Ortiz, J. V.; Cui, Q.; Baboul, A. G.; Clifford, S.; Cioslowski, J.; Stefanov, B. B.; Liu, G.; Liashenko, A.; Piskorz, P.; Komaromi, I.; Martin, R. L.; Fox, D. J.; Keith, T.; Al-Laham, M. A.; Peng, C. Y.; Nanayakkara, A.; Challacombe, M.; Gill, P. M. W.; Johnson, B.; Chen, W.; Wong, M. W.; Gonzalez, C.; Pople, J. A.; Gaussian 03, revision A.1; Gaussian: Pittsburgh, PA, 2003 .